FINAL REPORT, PHASE 2

ATOMIC HYDROGEN MASER FOR SPACE VEHICLE APPLICATION

July 1969

Contract NASW-1337

(March 31, 1968 to May 31, 1969)

Prepared by

HEWLETT hp PACKARD
Frequency and Time Division-East, Salem Road, Beverly, Massachusetts

for

NATIONAL AERONAUTICS AND SPACE ADMINISTRATION

Office of Space Science and Applications

Washington, D.C. 20546

Final Report -- Phase 2

Research Leading to the Development of an ATOMIC HYDROGEN MASER FOR SPACE VEHICLE APPLICATION

July 1969

Contract NASW-1337

Period Covered:
March 31, 1968 to May 31, 1969

Prepared by:
R. F. C. Vessot

HEWLETT-PACKARD CO.
Frequency and Time Division - East
Beverly, Massachusetts

for

NATIONAL AERONAUTICS AND SPACE ADMINISTRATION
Office of Space Science and Applications
Washington, D.C.

Table of Contents

TABLE OF FIGURES

I. INTRODUCTION

The following discussion covers a period of activity from March 31, 1968 to May 31, 1969, and is the second and final phase report for Contract NASW-1337. This report complements the Phase 1 Final Report for the period March 1, 1966 to March 31, 1968.

Essentially, the goals of the program have continued unchanged and consist of developing a hydrogen maser clock system suitable for use in a satellite. In particular, the first planned use of such a system is to verify the effect of gravitation on time as predicted by the principle of equivalence which is a cornerstone of Einstein's General Theory of Relativity. Refinements in the concepts of the experiment, notably in the use of an eccentric synchronous orbit, have increased the accuracy of the proposed experiment to 30 parts per million, since the stability as well as the accuracy of the clock now becomes useful.

Other uses for the clocks have been foreseen. One rather exciting application involves an extremely long baseline radio interferometer using two satellite-borne antenna and clock combinations. Correlation of data received would be performed at one or both stations and no data link involving radio noise signals would have to penetrate the earth's atmosphere. Data would be transmitted from satellite to satellite, and only the results of the cross-correlation of the signals would be transmitted earthward.

The clock system has been designed to be operable on the ground as well as in the space environment. Our early designs of components did not emphasize low weight or low power since the spacecraft then envisioned would accommodate both requirements. As the experiment plan evolved, it became very apparent that low weight and power were important, especially if a satellite exclusively for the relativity experiment was being designed.

There are many ground-based uses of the clock system, such as for satellite deep space doppler tracking, long baseline radio interferometry, and geodetic measurements using a satellite.

The work in this phase has been divided into four tasks.

Task I: Investigate wall coatings for the maser bulb and build and test a transistor oscillator exciter and r.f. dissociator.

Task II: Evaluate and test the mechanical and thermal design of the maser made under Phase 1 of the program; investigate improved cavity materials; establish mechanical and thermal specifications.

Task III: Establish a block diagram for the electronic components of the system. Build breadboard flight hardware models of the thermal and pressure controllers, phase lock system and r.f. dissociator exciter.

Task IV: Establish environmental and system specifications, and document a quality and reliability plan and an experiment operation plan.

The description of the work on these tasks will follow in the above order. The status of each task as of the termination date will be described in detail.

As a result of the decision of Hewlett-Packard not to engage in space equipment fabrication and a subsequent decision to move the Beverly, Mass. operation to Santa Clara, California, the NASA maser development activity will be transferred to the Smithsonian Astrophysical Observatory in Cambridge, Massachusetts. The work begun in the four tasks above will be completed at S.A.O. Equipment and personnel will be relocated in mid-June 1969, and operation on a new basis will begin July 1, 1969.

II. PROGRESS OF THE PROGRAM

A. Wall Coatings and R.F. Dissociator --Task I

Task I is advanced development work directed toward getting a more reliable and efficient r.f. hydrogen dissociator and to investigate, on a limited scale, the crystalline properties of TFE* Teflon in an effort to obtain a smaller, more constant frequency shift due to wall collisions in the bulb and to reduce the rate at which atoms recombine when they hit the wall. The currently used wall coating is made of melted films of FEP* Teflon. These cause a phase shift of about 10^{-5} radians per bounce with a probability of about one recombination every 10^{-4} bounces. Very little has been done either at universities or in industry prior to this contract to look for better coatings since the available coatings seemed adequate. Because the quality of the wall is the present chief limitation to the unperturbed storage time and consequently to the intrinsic stability of the maser oscillator, it is not unreasonable to expect to improve the maser substantially by working in this direction.

The specific approach in Task I is to coat bulbs with TFE Teflon, using the aqueous suspended material from du Pont, and to cure the Teflon so as to sinter it together and then cool it very slowly through the crystallizing range. The crystalline TFE Teflon should be far less porous than the amorphous TFE Teflon and the amorphous FEP. Further, since the TFE Teflon molecule is a single, long strand polymerized from carbon tetrafluoride and has some ten times the molecular weight of the FEP molecule that is multi-branched, there should be many fewer places for molecular end groups that harbor non-fluorine atoms. It is believed that the non-fluorine atoms, such as hydrocarbons that are loosely bound to the carbon-fluorine matrix, contribute both to the recombination rate of hydrogen and to the small variations in wall effect.

Sample films of TFE and FEP resin have been cast on the inside surface of 1-liter, round bottom pyrex flasks. The fast and slow temperature cycling technique has been used on TFE resin and the mechanical properties of the films have been tested.

* E.I. du Pont de Nemours trademark.

Fast-cured films, where the temperature went to 350°C and was dropped to room temperature within 5 minutes, show a rougher surface texture and coarser internal granularity than do films that have been sintered at 350°C and brought through the (340 - 295°C) crystallizing range at a rate of 0.5°C per minute. The mechanical properties seem similar. No difficulty in applying the TFE Teflon has been encountered, and a successive build-up of layers, each sintered in turn to the sublayer, is possible.

The degree of crystallinity of the TFE film can be measured by comparing the infrared absorption at 778 $cm.^{-1}$ (12.85 μ) and that at 2367 $cm.^{-1}$ (4.22 μ). The 778 $cm.^{-1}$ absorption is present only in the amorphous phase of the material, while the 12.85μ absorption is present in both the amorphous and crystalline phases. The ratio of the 778 to 2367 absorptions gives a measure of the absorption that is normalized to the film thickness and allows a precision of $\pm 1\%$ at 50% crystallinity according to C.A. Sperati and H. W. Starkweather in Advances in Polymer Science, Springer-Verlag, Berlin 1961.

The method has been tried and one set of absorption spectrograms of two films--one slow-cured, the other fast-cured--have been made. Judging from the over-all spectrogram from 5000 $cm.^{-1}$ to 650 $cm.^{-1}$, the slow-cured Teflon shows less amorphous absorption at 778 $cm.^{-1}$ than the fast-cured film. The 2367 $cm.^{-1}$ band on the one run showed an anomalous behavior that is most likely instrumental since the gain of the instrument was pushed up 5 times due to the thinness of the films. In future, several layers of film will be used in the sample, making the absorption stronger. The data now available indicates that the crystallinity of the films can be affected by the cure cycle. Future tests will be made to determine the extent to which the crystallinity affects the wall relaxation rate and the phase shift per bounce. To this end a bulb has been coated with TFE material and has been cured at the slow rate of cooling. It will be fitted in the NASA H-10 maser No. 6 and tested for relaxation rate and wall shift in a future phase of the program.

A part of the work on the r.f. dissociator has consisted of investigating various kinds of discharge tube materials, chiefly glasses, in an effort to find materials that will survive a long-term exposure to an atomic hydrogen plasma.

It was found that glass that contains metals such as lead, potassium or sodium performs badly due to the reduction of metal oxides, leaving free metal surfaces that are catalysts for hydrogen recombination. Borosilicate glasses such as Corning's Pyrex 7740 and 7070 work well. An important reduction of the rate of erosion of glass due to the discharge can be obtained by exciting the discharge by magnetic rather electric excitation since the electron motion is circular rather than towards electrodes outside the glass. Further improvement results from applying a d.c. magnetic field to confine the electrons. This field, chosen roughly at the proper level to match the cyclotron frequency to the excitation frequency, helps to extend the trajectories of the electrons even though the mean free paths are only comparable to the dimensions of the discharge tube.

A sketch of the r.f. discharge assembly is shown in Figure 1. The source that was tested on the vacuum stand and a potted set of electronics for the discharge are illustrated in Figure 2.

Several single-transistor oscillator circuits that have resonator coils made to surround the discharge tube have been designed. The basic circuit is shown in Figure 3.

Cooling the glassware that encloses the discharge is a problem. It is estimated that about one-half the input power is dissipated on the walls of the glass, and this can amount to ten watts. Several schemes were tried involving immersing the circuit and coil in viscous silicone fluid using the thermal conductivity--not the convection--to provide cooling to a set of thermally conducting posts leading to an outside heat sink plate of the maser. The presence of the fluid causes a little dielectric loss; however, it does cause dielectric loading that increases the distributed capacity in the coil. Fortunately, the coil and its series resonant capacitor are driven at a low level of impedance; and since we desire to excite the discharge magnetically, the coil can be designed so that the increased capacitance does little to reduce the r.f. magnetic fields in the discharge. This type of discharge was tested on a vacuum stand, and the scheme of using a conducting fluid seems feasible. The efficiency of the discharge, judged from its brightness vs. the amount of power consumed, is somewhat reduced by using the fluid. However,

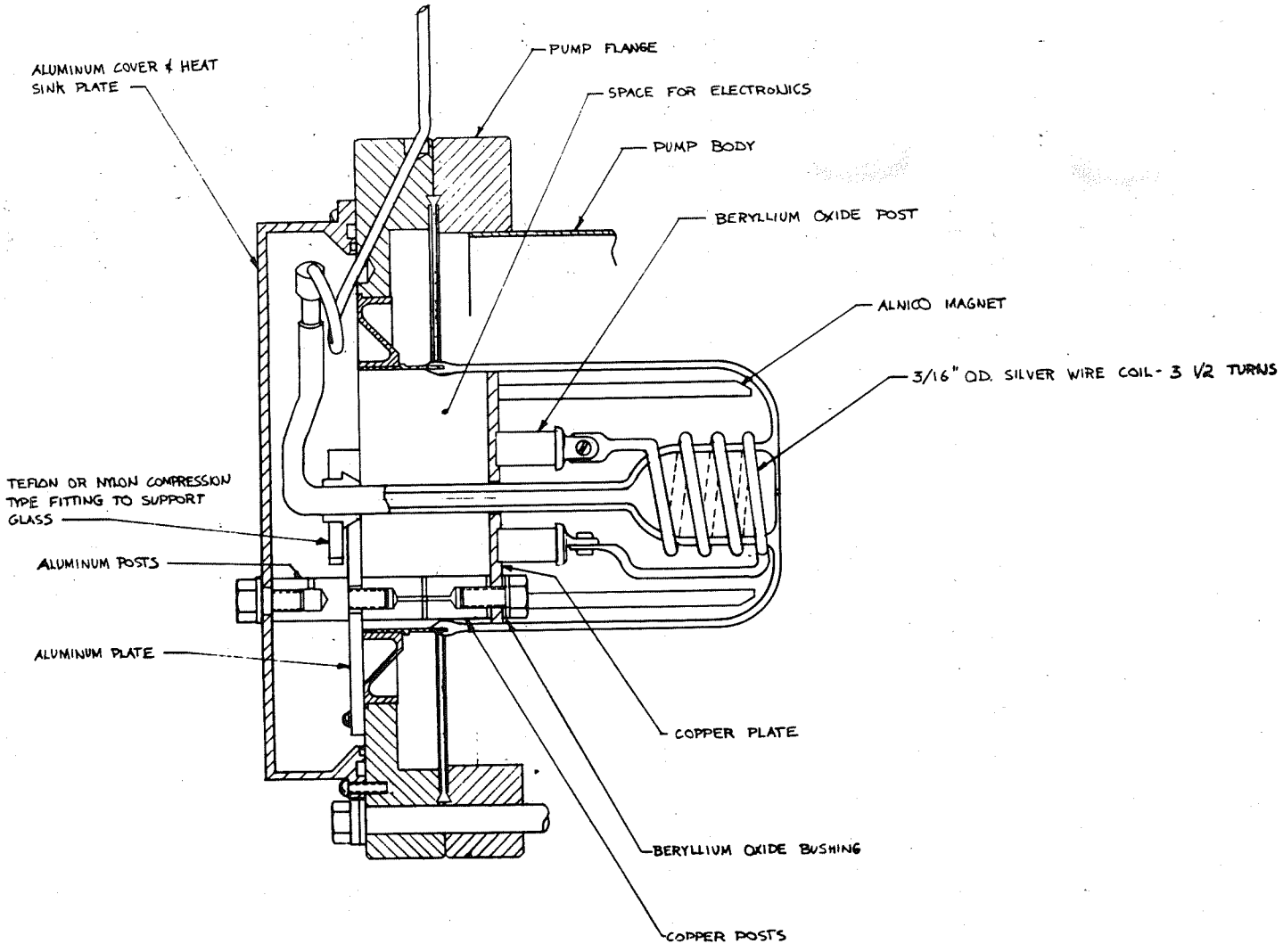
ALUMINUM COVER & HEAT SINK PLATE
PUMP FLANGE
SPACE FOR ELECTRONICS
PUMP BODY
BERYLLIUM OXIDE POST
ALNICO MAGNET
3/16" O.D. SILVER WIRE COIL - 3 1/2 TURNS
TEFLON OR NYLON COMPRESSION TYPE FITTING TO SUPPORT GLASS
ALUMINUM POSTS
ALUMINUM PLATE
COPPER PLATE
BERYLLIUM OXIDE BUSHING
COPPER POSTS

Figure 1.

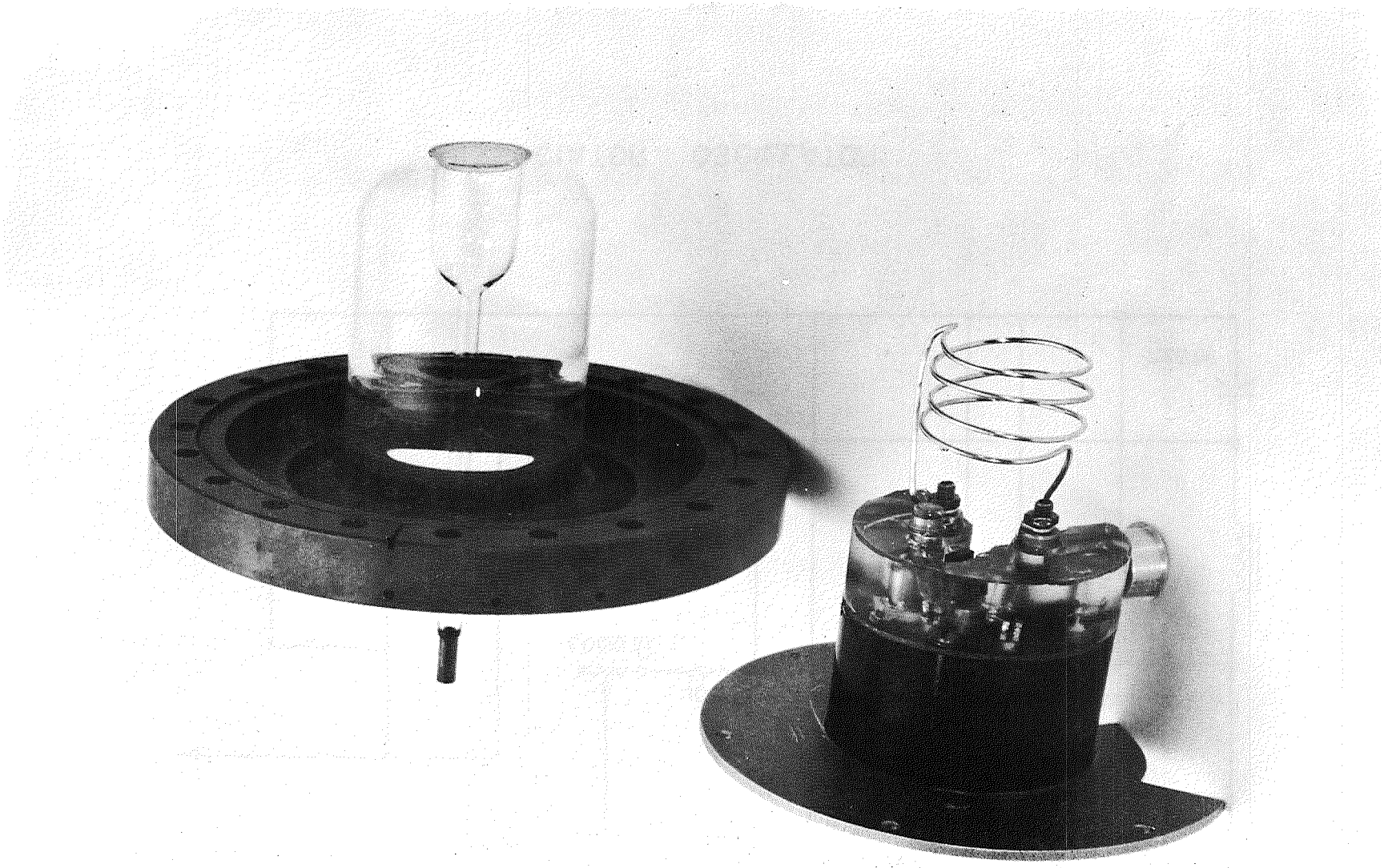

Figure 2.

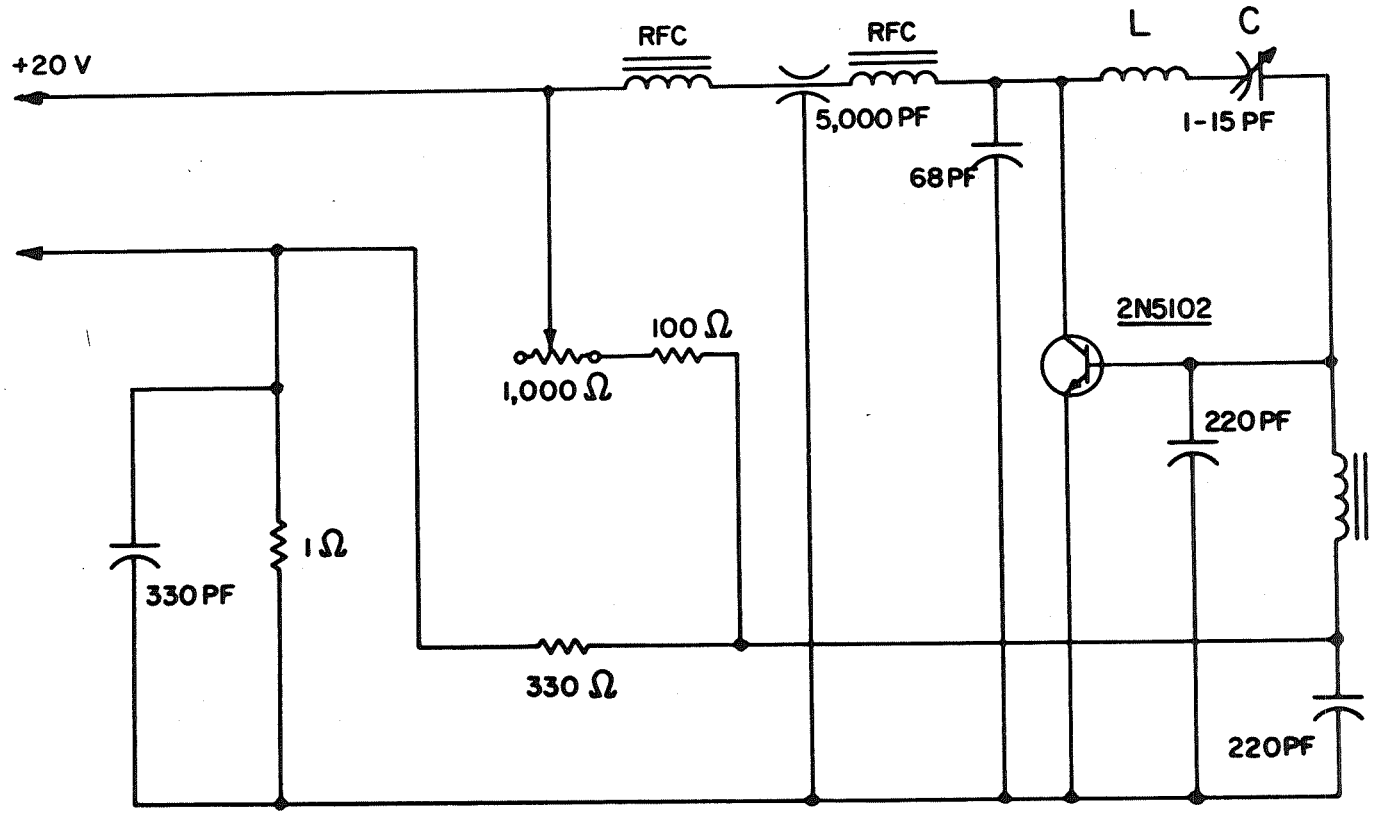

DISSOCIATOR OSCILLATOR

Figure 3.

the use of the fluid thermal conductor seems to be a good way of making intimate thermal contact with the glass without subjecting it to mechanical strain or electromagnetic perturbation.

By modulating the amount of power into the discharge, it is possible to modulate the degree of dissociation of the molecular hydrogen in the discharge tube. This offers a means of rapidly varying the atomic hydrogen beam flux into the maser bulb, a process that is necessary for tuning the maser cavity. Since the flux variations can be made rapidly, one can use a less stable reference than a maser oscillator tuning.

The variable power supply for operating the discharge is similar in operation to the pulse-duration thermal and pressure controllers which are discussed later under Task III.

B. Mechanical and Thermal Design, Cavity Design, Thermal and Mechanical Specifications -- Task II

1. Mechanical Testing

The feasibility of making a small maser having been proved in Phase 1 of NASW-1337, the work of designing a maser mechanically and thermally suited for satellite application was begun. From a mechanical testing point of view, it is convenient to divide the package into three parts. First and most critical is the cavity-bulb assembly; second is the oven and magnetic shield assembly and vacuum envelope enclosing the cavity; third is the vacuum pump, magnetic state selector, r.f. dissociator and gas-handling assembly.

The cavity-bulb assembly has been vibration-tested axially and transversely at three levels of sinusoidal excitation:

Phase A	5-16 Hz at 0.040 inch, double amplitude 16-2000 Hz at 0.5 g, peak acceleration
Phase B	5-16 Hz at 0.15 inch, double amplitude 16-2000 Hz at 2 g's, peak acceleration
Phase C	5-16 Hz at 0.30 inch, double amplitude 16-2000 Hz at 4 g's, peak acceleration

The conclusions drawn from this test are as follows:

1. The vertical and lateral axes testing data obtained thus far tends to indicate that maser design is compatible with the sinusoidal vibration environments to which it has been subjected.

2. Three design changes were deemed necessary:
   a) The cylindrical cavity is to be fastened to the bottom ring with epoxy.
   b) The expansion posts should be isolated with soft copper washers.
   c) Pre-load on the cavity should be increased.

3. All major vertical and lateral axes resonances are in the higher frequency domain--i.e., greater than 200 Hz.

The details of this vibration testing are given in Appendix I, which is a report on the work done by the Vibration and Acoustics Branch of the Propulsion and Vehicular Engineering Division of the NASA Marshall Space Flight Center.

2. Redesign of Ion Pump

Extensive revision of the design of the ion pump has taken place to make the device lighter, more rugged, and more easily assembled and tested. The pump also has been shortened. Improved access to the relocated vacuum feed-through for the r.f. and the vacuum header for the electrical connections leading to the Zeeman coil and the electronic tuning diode has been provided. The pump is shown in Figure 4. It will be noticed that the heavy base flange is still present. It will remain in the design until a later stage of flight hardware prototype design, when the heavy flange joint will be replaced by a weld; this will result in a saving of about 12 lbs.

The magnet structure for the pump has been redesigned and lightened by reducing the amount of magnetic material by at least 35 lbs. As seen in Figure 4, where one of the six segments is shown in place, the keeper between the magnets is made of Armco iron sheet. The field in the magnet gaps where the pumping elements are located now averages about 800 gauss and is ample for ion-pumping hydrogen.

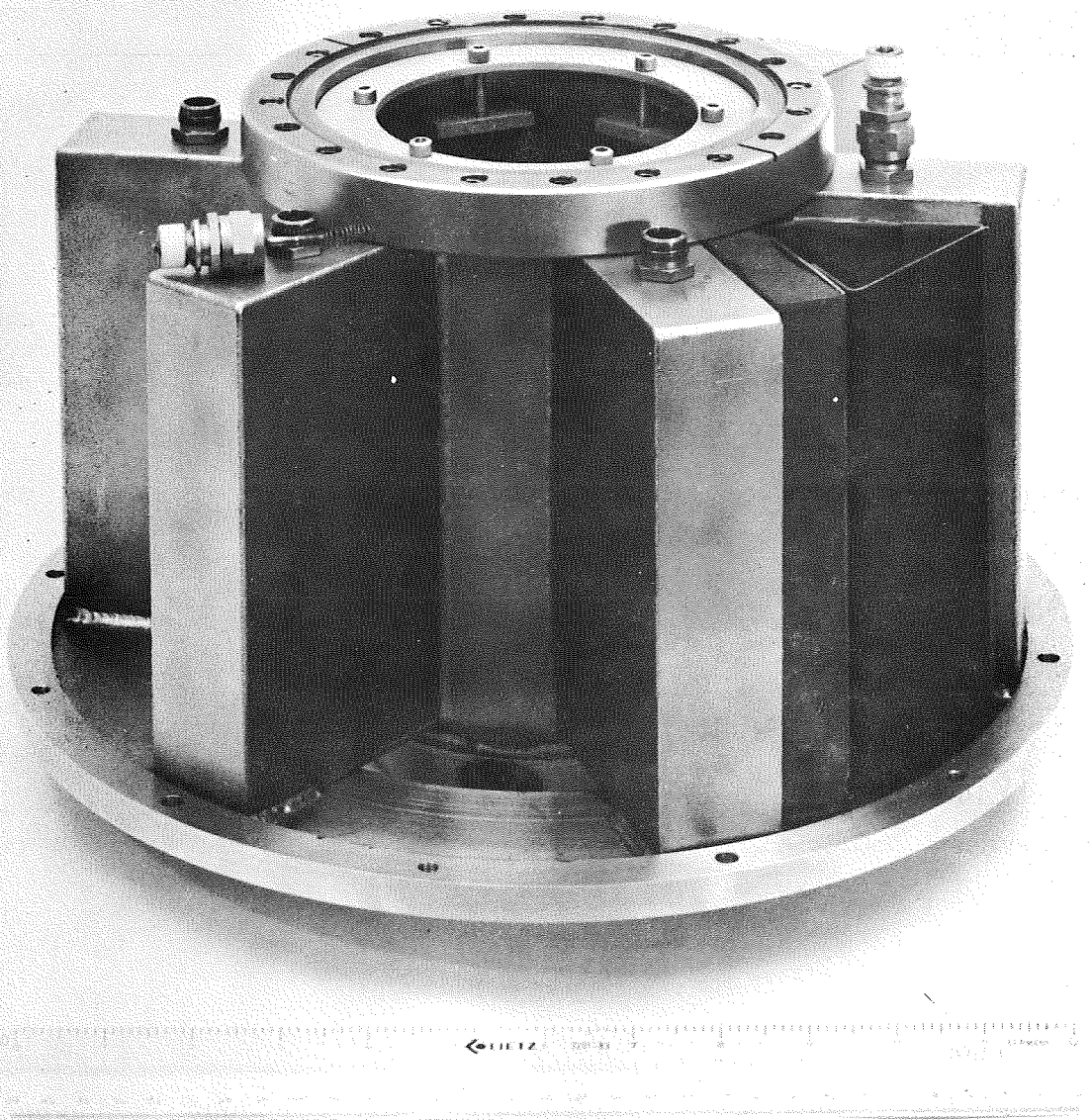

Figure 4.

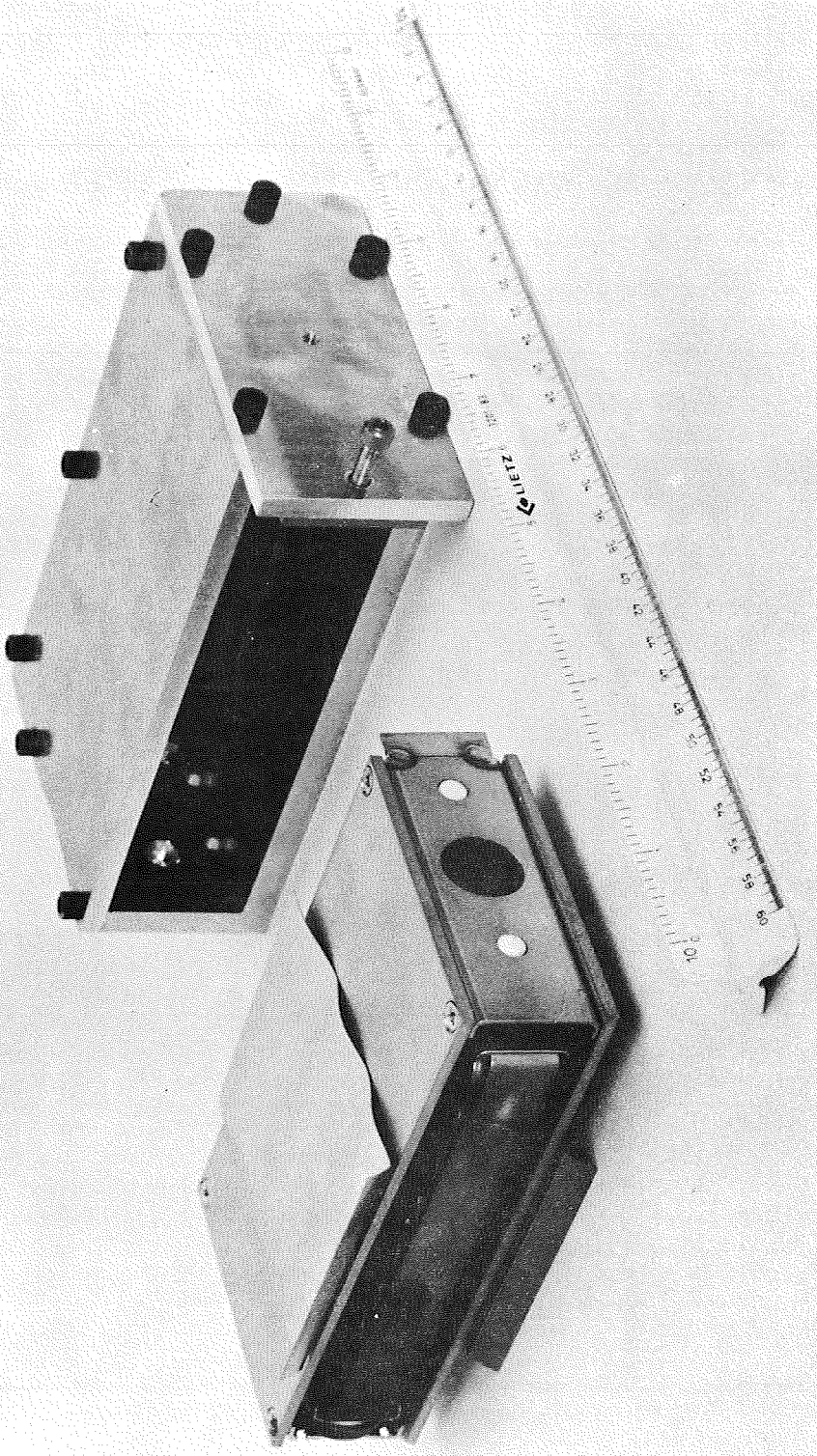

Figure 5.

Changes in the design of the pumping elements have been made, and diagnostic vibration has been done to verify the design. The elements, shown in Figure 5 with the testing fixture, consist of a structure where a multi-celled anode is placed between two titanium plates. The anode must be insulated to at least 5 kV while under vacuum. To get the anode rigidly mounted between the cathodes, four pre-loaded Bellville-type washers have been used, one on each of the insulating alumina posts. The anode structure is under about 150 lbs. compressive load. Stiff mounting of the six elements in the vacuum envelope has been accomplished by axially loading each element by a toggle clamp. Sideplay and lateral vibration modes of the titanium plates have been taken out by the use of thin corrugated plates inserted between the titanium anodes and the stainless steel vacuum envelope.

3. Redesign of Beam Optics System

A major redesign of the atom source and hexapole magnet mounting structure has been done. The chief considerations are to have a rigid, accurate positioning of the magnet along the pump axis and still allow ample pumping speed. Furthermore, the r.f. discharge should be shielded to prevent r.f. leakage from the discharge getting out of the ion pump via the high voltage leads. The structure is shown in Figure 6. It is a stacked array that, starting from the midriff end of the pump, consists of the following:

1. A three-legged spider structure that is centered in the pump and holds the magnet.
2. The hexapole magnet.
3. A second three-legged spider that encloses a thin stainless steeel dome that encloses the end of the discharge tube; this dome has a hole on its axis to let out the beam of atomic hydrogen.
4. A stainless steel cylinder.
5. A mating ring to align the stainless steel cylinder into the Bellville washer that provides an axial pre-load of about 100 lbs.
6. The Bellville washer is seated in a ring that is caught in the source flange shown in Figure 2.

By fastening the source flange and pulling the bolts up against the tension of the washer, one can get the source firmly fastened and accurately aligned on axis.

Figure 6.

4. Neck and Heat Station

From experiments on a similar maser structure built under NAS8-2604, it was found that the neck leading to the bell jar caused an appreciable thermal gradient in the jar--enough to affect the thermal compensation required to offset the temperature coefficient of dielectric constant of the fused silica bulb that is located in the resonant cavity. For this reason, the neck was redesigned to include a heat station. As shown in Figure 7, the neck includes two vacuum joints and two bellows sections joined to a center piece that is kept at constant temperature by monitoring via a thermistor and supplying heat from a temperature servo circuit. A copper constantan thermocouple is included to allow a rough measurement of the temperature.

5. Midriff Structure

The pump with its magnetic shields is fastened to a midriff plate shown at the bottom of the stack of discs in Figure 8. The midriff plate is the main mounting structure for the maser. It will be made of titanium for strength, light weight, and avoidance of magnetic effects. The present version is made of aluminum and serves as a mock-up for assembly and electronic testing. All the electrical connections will be included in the midriff.

6. Ovens and Shields Assembly

In order to enclose the vacuum bell jar in a structure having a low-field, isothermal temperature of 50°C, a multiple oven - magnetic shield combination is required. To provide the uniform, axial magnetic field in the bulb, a solenoid is wound close to the inside of the innermost shield. This solenoid is made in four windings: a main winding, two end windings, and a Helmholtz array. In theory the end windings take out second-order axial gradient at the bulb center and the Helmholtz array takes out residual fourth-order gradients.

Structurally, this array of solenoid, four magnetic shields and two ovens is a problem. We want to maintain the axis of the bell jar and base aligned to the axis of the pump without making thermal leakage paths that would cause temperature gradients. We also have to support the thin moly-permalloy shields so as to

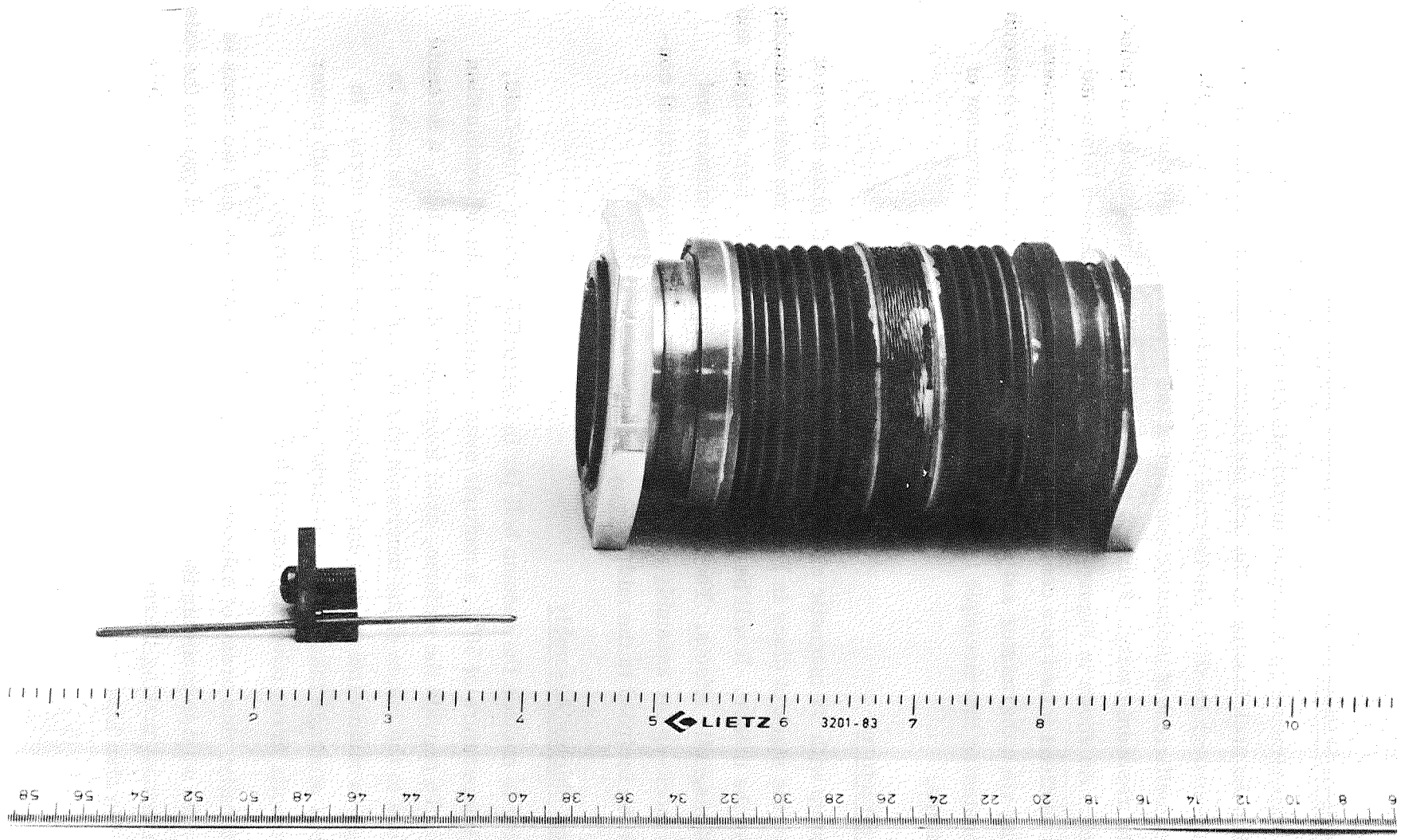

Figure 7.

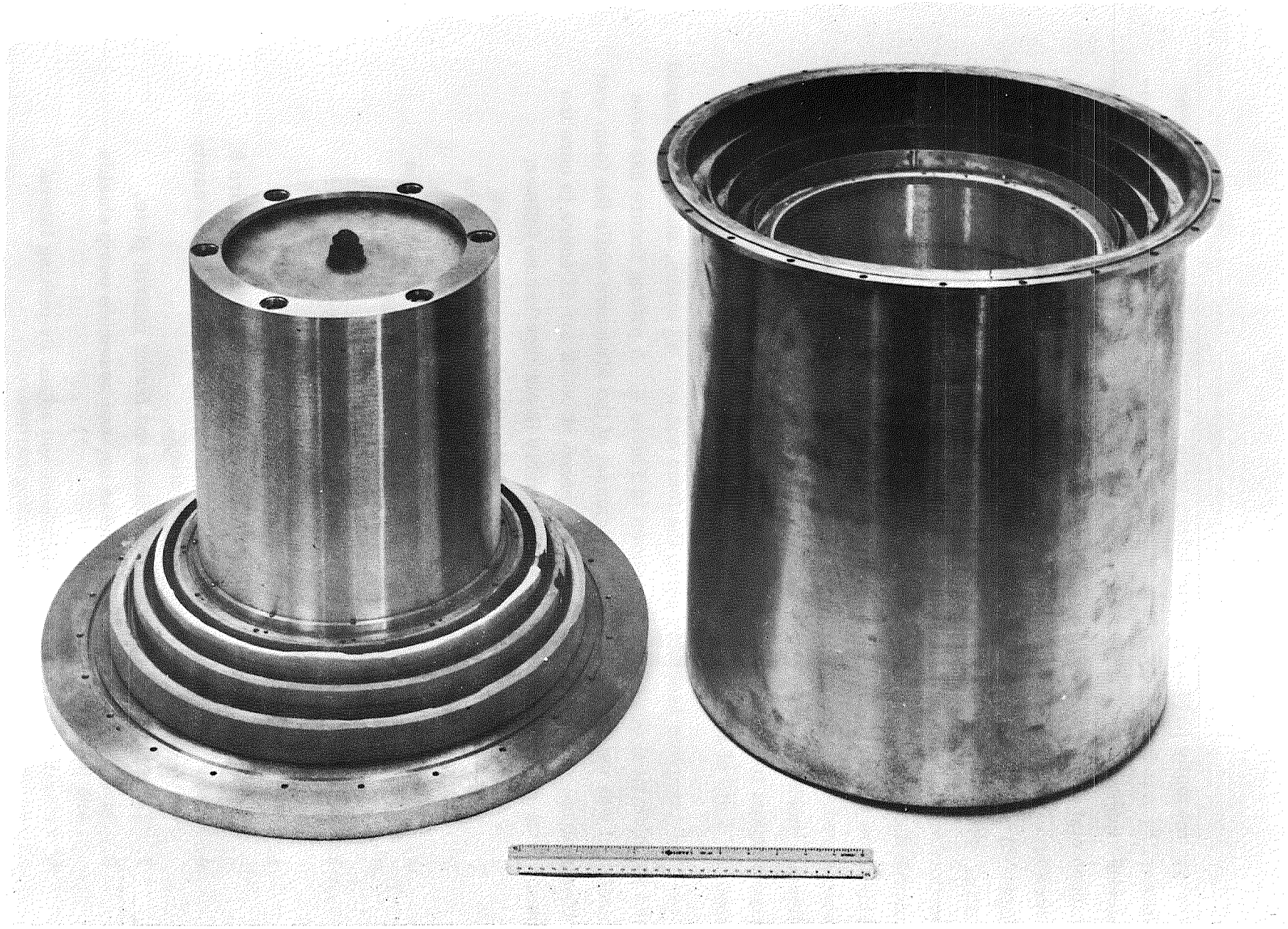

Figure 8.

prevent magnetic hardening from deformation. Furthermore, we must have no dissimilar metals in electrical contact with each other so as to prevent thermo-electric currents resulting from thermal differences in dissimilar metals. The expansion between magnetic shields and oven isothermal enclosures has been taken up by coiling Teflon tubing about the cylindrical shields and pressing them (lightly!) into the aluminum isothermal supports. This also insulates electrically. The corresponding end caps are insulated by 0.010" mylar sheet. To support and insulate the successive layers, it was decided to use an epoxy, microballoon foam that does not change dimensions appreciably on curing. This foam weighs 14 lbs./cu. foot and has a compressive strength of 150 psi when cured. Measurements of the thermal properties of the foam on a full-size thermal mock-up give a conductivity figure of 7×10^{-4} watts/cm^2/^{0}C. It is expected that to cope with the lowest ambient specified--i.e., 20^{0}C--it will take about 25 watts of power into the ovens if the present design concept is used.

The complete assembly using the foam and with all ovens, shields, solenoid and the electrical connections is shown in Figure 8. A potting fixture has been made and was used to maintain the alignment of the structure while the foam was being poured. The whole assembly was baked at 300^{0}F for 48 hours to cure the foam. The midriff and bell jar base assembly is put together as follows:

1. Assemble the cavity while mounted on the base plate - neck assembly. Lead out Zeeman wires, r.f. output coax and the tuning diode wires to the heat station in the neck.
2. Test the cavity while under vacuum using a test bell jar. (The jar to be used in the maser is "potted" in the assembly of shields and ovens.)
3. Assemble the base plate with the neck and cavity onto the jar and tighten the vacuum joint.
4. Vacuum test for leaks.
5. Assemble, piece by piece, the stacked array shown in Figure 8.
6. Determine shim thickness to get a 300 lb. pre-load on the cavity base, and place shim on top of stack.
7. Lead out all electrical connections and fasten midriff plate.
8. Invert structure so pump end is up, and assemble pump shields and pump.
9. Check pump and cavity alignment and adjust by making lateral adjustment in the pump mounting hardware.

10. Connect leads through the neck heat station to the appropriate header connections inside the pump.
11. Install hexapole magnet assembly shown in Figure 6.
12. Before bolting in the source plate, check alignment of hexapole magnet, stopping disc and bulb entrance aperture.
13. Assemble source plate providing pre-load for holding the stacked array containing the magnet.
14. Assemble ion pump shields.

7. Mechanical Vibration Testing Plan and Specifications

The original plan to vibration-test the maser assembly was to make two shake fixtures shaped like the two sides of the midriff. The cavity assembly and the pump assembly would be tested separately, each under a rough vacuum. Accelerometers would be placed at the crucial locations and led out of the vacuum envelope through the neck using a special header. The levels of testing are given in a separate document, "Preliminary Development and Test Planning Document for S081 Redshift Relativity Experiment Program Planning Document." The latest version of this is dated October 16, 1968 and was drawn up in collaboration with NASA Marshall Space Flight Center. This document, in an abbreviated form, is included in the "Preliminary Project Development Plan for the Hydrogen Maser Relativity Satellite" dated November 5, 1968, that was prepared in collaboration with NASA Marshall Space Flight Center.

Concurrently with the subject contract there has been a program (contract NAS8-2604) for development of a small ground-based maser unit using the design of the satellite maser oscillator as a basis. This small maser has been fitted with a Cer-Vit cavity in place of the fused silica formerly used. The advantages of Cer-Vit over fused silica are due to its 30 times smaller coefficient of thermal expansion. Much was learned from this work and can be briefly summarized as follows:

1. The heavy silver coating on flat plates can deform the plates due to thermal stressing.
2. Fused silica as used in the bulbs has a not-negligible thermal coefficient of dielectric constant.

3. It is possible in a well controlled way to compensate the cavity such that the coefficient of resonance frequency with temperature is less than 100 Hz/^{0}C.

4. Thermal gradients must be well controlled if the compensation is to be effective.

C. Block Diagram and Electronic Breadboards -- Task III

The experiment system block diagram has been completed. This diagram shown in Figure 9, includes two separate areas of responsibility with a well defined interface. These are defined as the clock system and the telemetry system. The clock system includes the two masers, their supporting electronics, the phase-lock system and the autotuner system. The telemetry system includes the doppler cancelling transponder, the clock signal transmitter, power supplies and all command and telemetry systems. Command and telemetry requirements for the experiment have been established and are included in a preliminary project development plan prepared by NASA-Marshall.

The development of flight hardware breadboard models of the thermal and pressure controllers has been begun and the thermal breadboard is ready for testing. The breadboard of a typical thermal control circuit is shown in Figure 10. The circuit using a self-oscillating bridge and pulse-duration control of power is shown in Figure 11. A similar power control circuit was used for the r.f. discharge.

Further measurements of frequency stability have been made, and the major sources of excess phase instabilities have been traced to the frequency multipliers. The data shown in Figure 12 are taken with the schematic shown in the same figure. Agreement with theory is quite good for averaging time intervals from 1 to 100 seconds. The major contribution to instability in this region is due to white thermal noise coming into the receiver (or due to its noisy first stages) and being added to the maser signal. In principle this effect should give T^{-1} behavior. The effects of other noise processes causes the data to flatten beyond about 100 seconds at an rms fractional frequency deviation of 7×10^{-14}. These other noise processes are causal, not thermodynamic, and can be improved by better mechanical, thermal and electronic design as well as by improvements in the storage ability of the bulb.

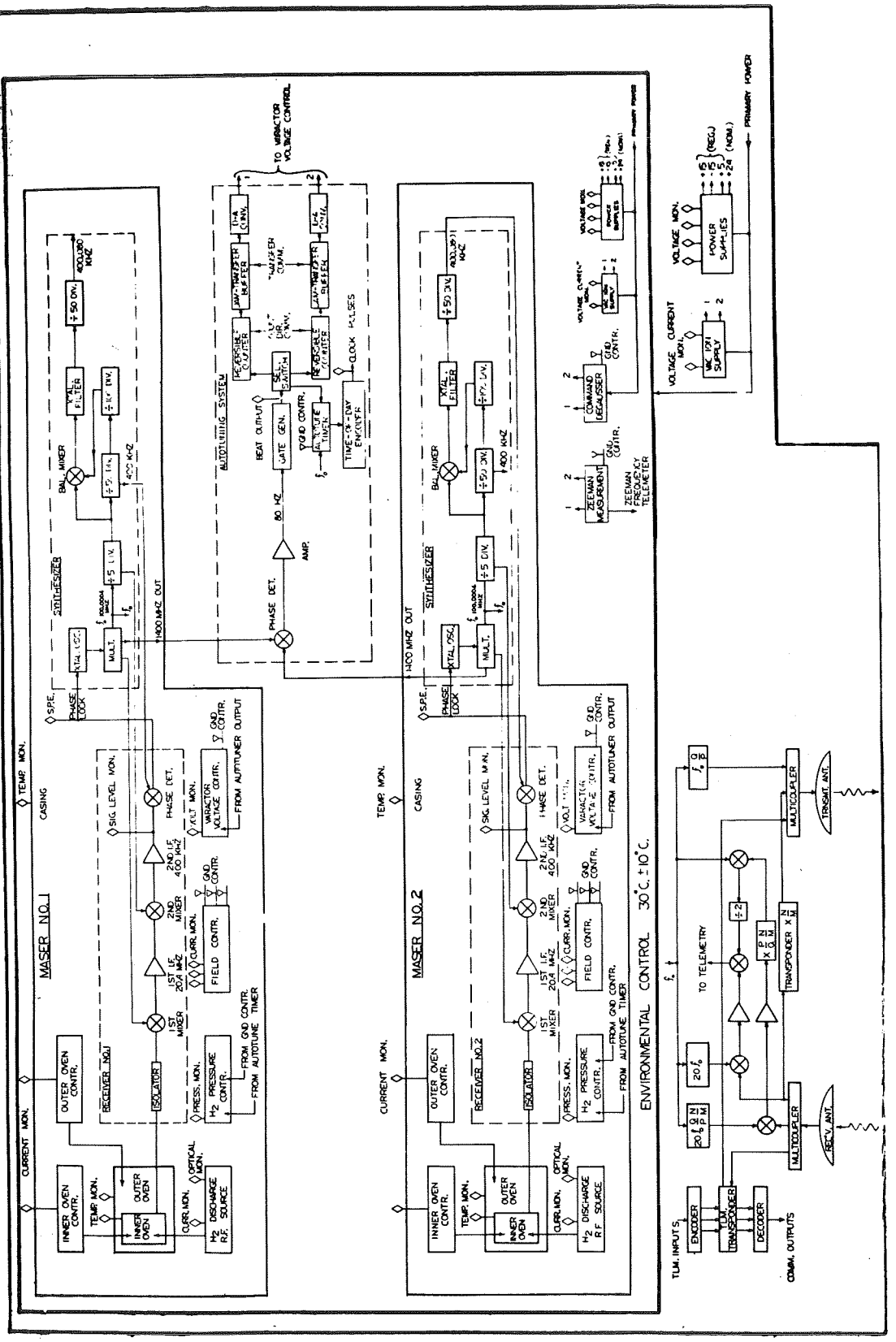
MASER NO.1
MASER NO.2
ENVIRONMENTAL CONTROL 30°C. ± 10°C.
SYNTHESIZER
AUTOTUNING SYSTEM
TO VARACTOR VOLTAGE CONTROL
TO TELEMETRY
TEMP. MON.
CASING
CURRENT MON.
OUTER OVEN CONTR.
INNER OVEN CONTR.
OUTER OVEN
INNER OVEN
H2 DISCHARGE R.F. SOURCE
OPTICAL MON.
ISOLATOR
1ST MIXER
1ST I.F. 20.4 MHZ
2ND MIXER
2ND I.F. 400 KHZ
PHASE DET.
SIG. LEVEL MON.
VOLT. MON.
VARACTOR VOLTAGE CONTR.
GND. CONTR.
FROM AUTOTUNE OUTPUT
FIELD CONTR.
H2 PRESSURE CONTR.
PRESS. MON.
FROM GND CONTR.
FROM AUTOTUNE TIMER
S.P.E.
PHASE LOCK
XTAL OSC.
MULT.
BAL. MIXER
XTAL FILTER
400 KHZ
80 HZ
AMP.
GATE GEN.
BEAT OUTPUT
PHASE DET.
VARACTOR BUFFER
VARACTOR COMM.
SEC. COUNTER
CLOCK PULSES
TIME-OF-DAY ENCODER
ZEEMAN MEASUREMENT
ZEEMAN FREQUENCY TELEMETER
COMMAND DECAUSSER
VOLTAGE MON.
VOLTAGE CURRENT MON.
VAC ION SUPPLY
POWER SUPPLIES
PRIMARY POWER
TLM. INPUTS
ENCODER
TLM. TRANSMITTER
DECODER
COMM. OUTPUTS
MULTICOUPLER
TRANSMIT ANT.
RECV. ANT.
TRANSPONDER

Figure 9.

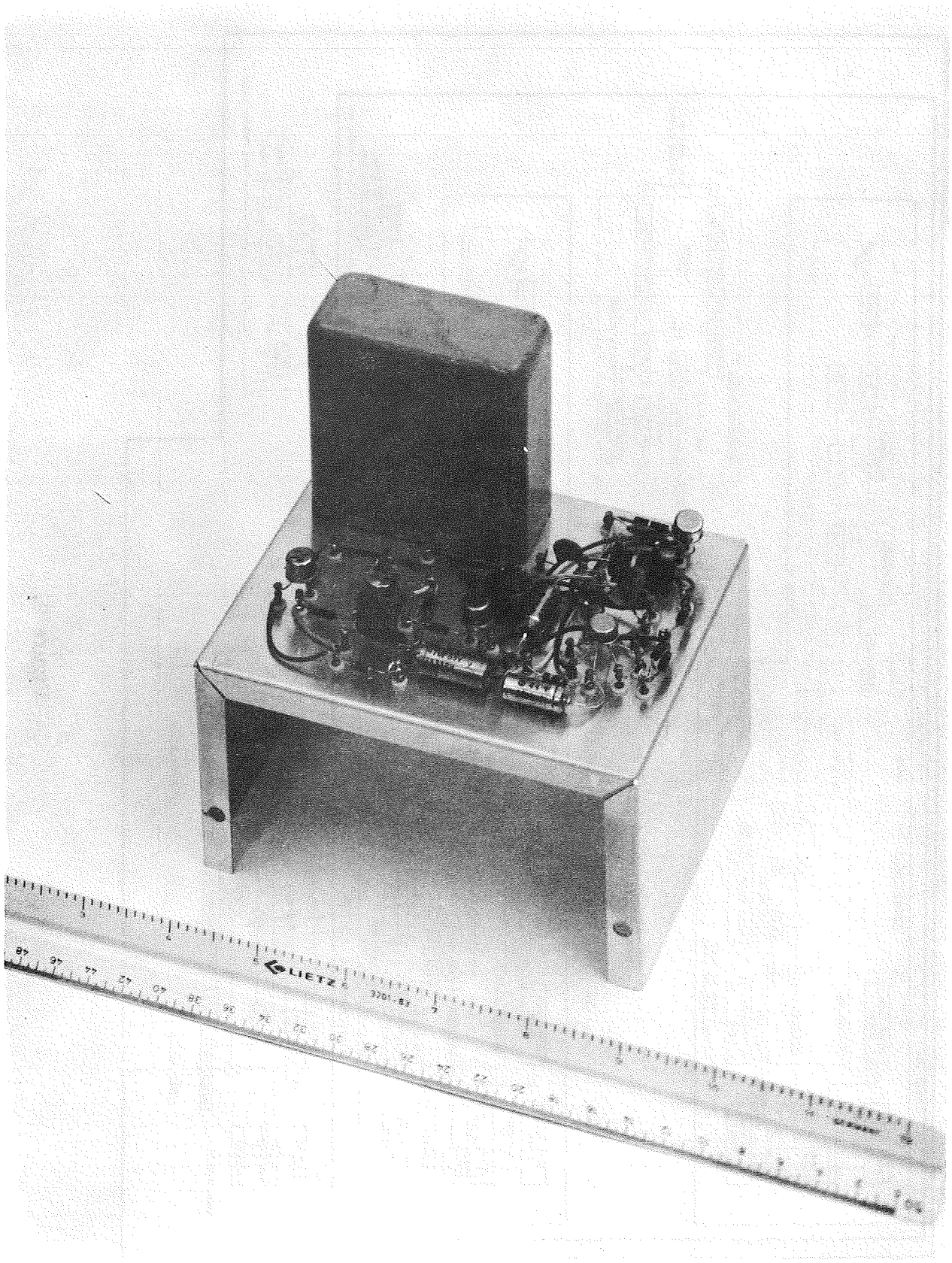

Figure 10.

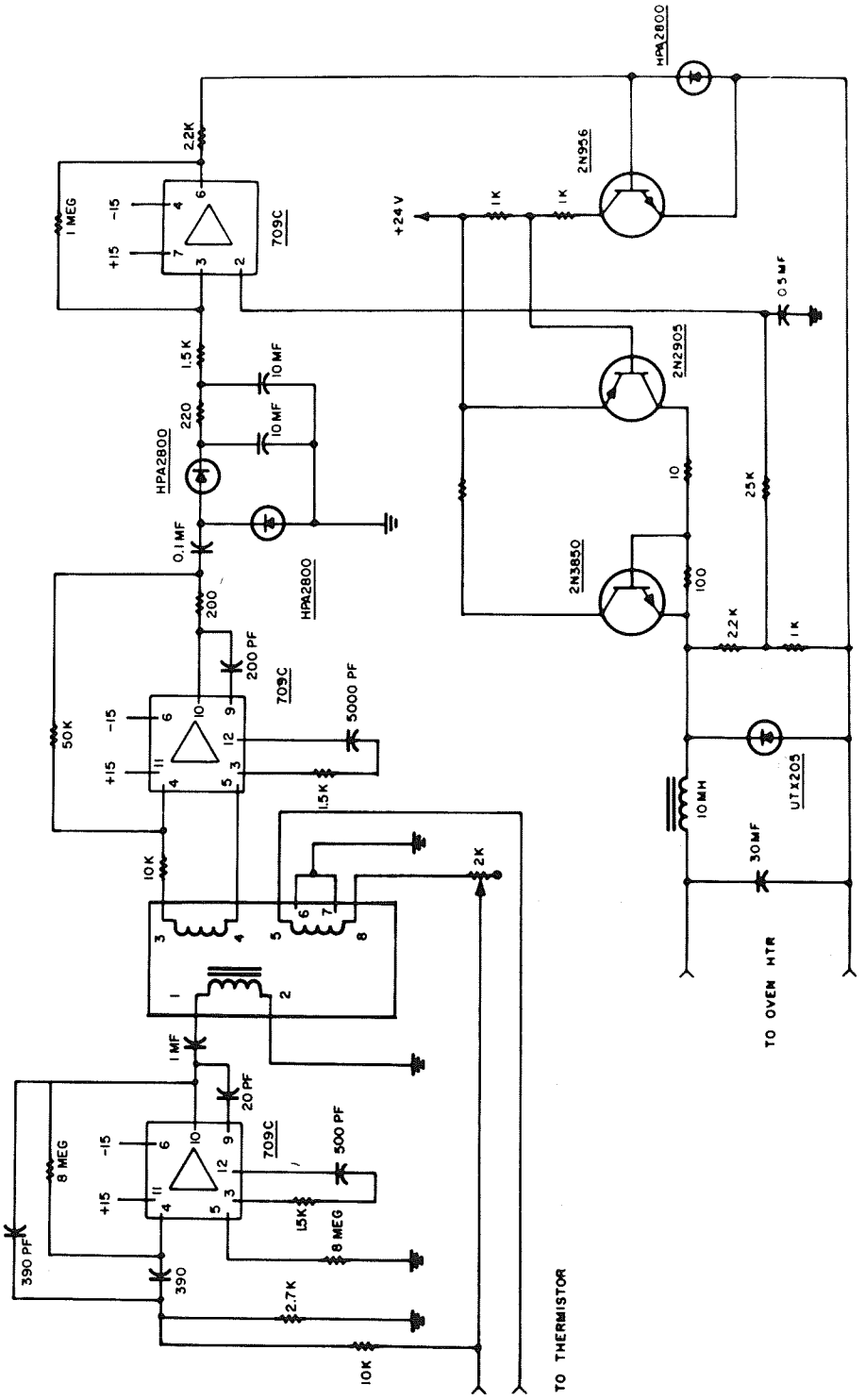
HPA2800
2N956
+24 V
1K
1K
2.2K
1 MEG
-15
+15
709C
0.5 MF
2N2905
1.5K
10 MF
10 MF
220
HPA2800
10
25K
2N3850
100
0.1 MF
200
HPA2800
2.2K
1K
200 PF
709C
5000 PF
50K
-15
+15
1.5K
10K
2K
10 MH
UTX205
30 MF
TO OVEN HTR
1 MF
20 PF
709C
500 PF
8 MEG
-15
+15
1.5K
8 MEG
390 PF
390
2.7K
10K
TO THERMISTOR

Figure 11.

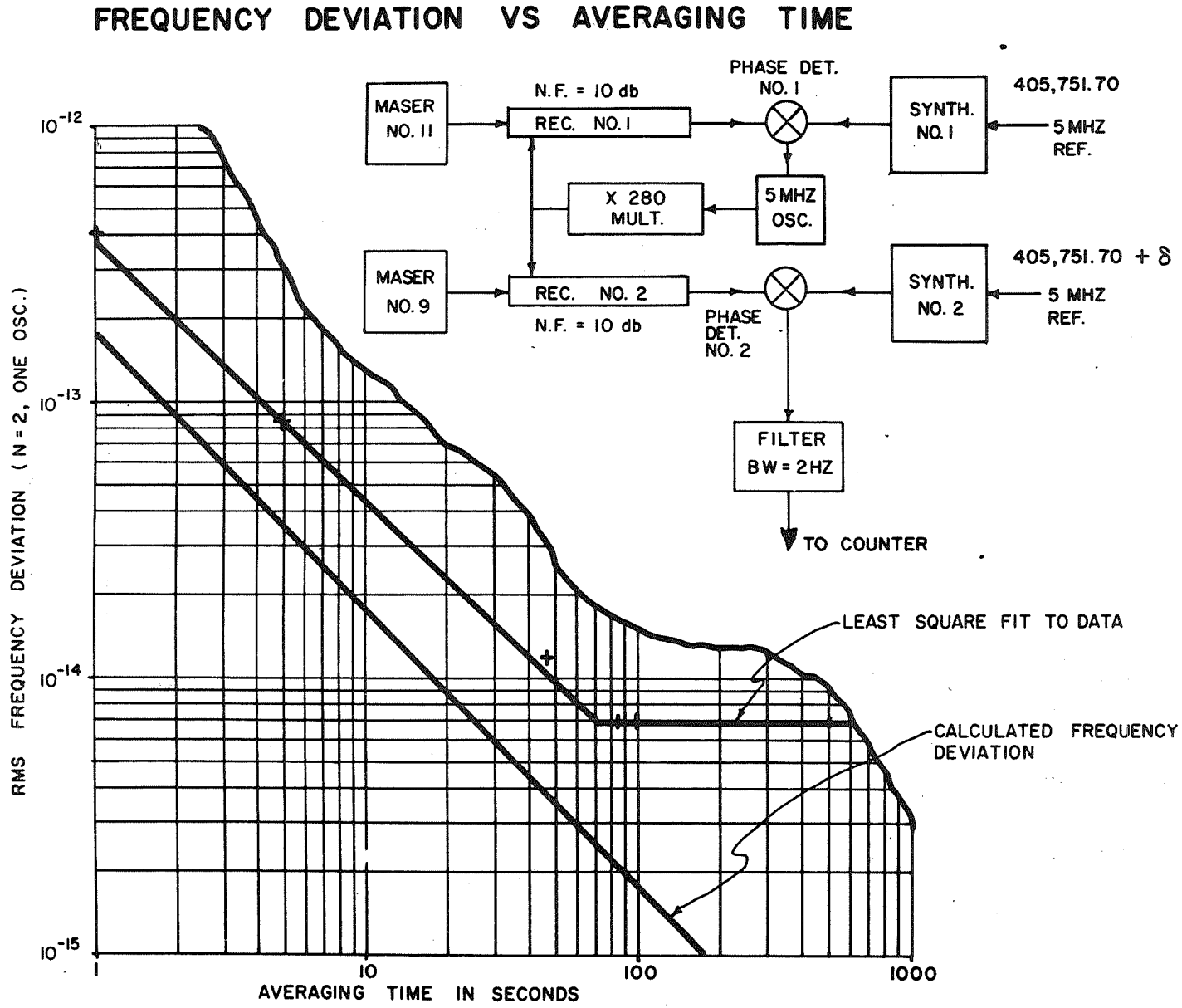
FREQUENCY DEVIATION VS AVERAGING TIME
MASER NO. 11
N.F. = 10 db
REC. NO. 1
PHASE DET. NO. 1
SYNTH. NO. 1
405,751.70
5 MHZ REF.
X 280 MULT.
5 MHZ OSC.
MASER NO. 9
REC. NO. 2
N.F. = 10 db
PHASE DET. NO. 2
SYNTH. NO. 2
405,751.70 + δ
5 MHZ REF.
FILTER BW = 2HZ
TO COUNTER
LEAST SQUARE FIT TO DATA
CALCULATED FREQUENCY DEVIATION
RMS FREQUENCY DEVIATION (N = 2, ONE OSC.)
10^-12
10^-13
10^-14
10^-15
1
10
100
1000
AVERAGING TIME IN SECONDS

Figure 12.

D. System Specifications, Quality and Reliability Plan, Experiment Operation Plan -- Task IV

The environmental specification is a software and documentation task that depends on a great many inputs relating to specific vehicles, orbits, and ground station conditions. At this time very incomplete information on these is available. Specifications of vibration, acoustic noise levels and thermal conditions have been estimated in a very general way, and a testing plan has been written with the aid of NASA-Marshall.

A draft of a quality assurance plan has been produced jointly by NASA-Marshall and Hewlett-Packard.

A great deal of revision in these documents will be required when the mission requirements, ground station locations, vehicle requirements and a host of other details become clearer.

1. Satellite Maser Experiment Operation Plan

A first cut at an experiment operation plan is given in Appendix II. Many assumptions have been made in drafting this plan. These involve the status at which the experiment begins and the configuration of orbit.

1) The satellite maser clock system is aboard the vehicle.

2) The satellite maser clock system and the ground clock system can be compared without intermediate clocks or traveling clocks.

3) The orbit is eccentric and allows constant phase tracking by the ground station that is near the launch site because of the above assumption.

4) Satellite maser clock system and ground clock system are electronically alike and can be controlled from a console at the ground station.

5) Recording of data is performed in three ways:

   a) Raw data from all telemetry on wide band F.M. recorders; this provides a sort of "archive" for the experiment.

b) Operating data is being recorded on strip charts to allow a quick look at the status of various parameters. (Preset levels of certain parameters will set off an alarm if these levels are reached.)

c) Digital form suitable for computer input.

6) Computer programs and computing facilities are available and accessible on short notice. These are used for data evaluation during the experiment.

7) Telemetry and command are under local control so as to minimize the delay in operating the satellite maser equipment.

8) Satellite tracking is continuously available on a separate system and this data can be obtained in up-to-date form during the experiment to provide "bench marks" for the phase-lock tracking system.

9) It is assumed that the experiment will last about two months and that a decision can be reached on the basis of the data received, whether to continue taking data either to improve the accuracy of the measurement or to look further into unexpected interesting effects that may result from the experiment. This requires that data reduction be accomplished within weeks of the obtaining of the data.

10) Three masers are assumed to be on board. In the course of development of the program it is possible that two masers and a high stability crystal oscillator or even three masers and a high stability crystal oscillator will be used.

Data Acquisition and Reduction -- After the checkout and tuning procedures have been performed as in Appendix II, the experiment is in a steady-state condition; the masers are tuned as well as possible and some knowledge of the systematic variations over the orbit is on hand. The data is presumed to be recorded in at least three forms, as discussed in (5) above.

A continuous digital representation of satellite range as a function of time can be used to determine the orbit once a value for initial position angles and radial distance is given. The computer program that will determine the orbit from this data will have to include the effects of the shape of the earth, the moon and

the sun, and the time dependence of these effects as the experiment proceeds. The orbital parameters such as apogee, perigee, line of nodes, etc., will be time dependent and will be determined on a best-fit basis using the telemetry range data and whatever other tracking data is available. From this "best fit" orbit it will be possible to obtain the predicted satellite clock system frequency shift. The measured clock frequency shift data comes from two sources: ground-based comparisons and satellite-based comparisons. It will be recalled that the two-way Doppler cancelling technique takes a running time average of the phase variations in the go-return path, divides the phase variation by two, and subtracts this from the phase of the clock carrier signal. If for some reason there are asymmetries in the velocity of propagation, the one-way phase variation will not be the average of the two-way phase variation. For this reason, similar data is also recorded aboard the satellite. The average value of the data will remove any possible asymmetries in the propagation.

These variations in the atmosphere will be interpreted as variations of range by the ranging system. The net effect of the atmosphere at nearly grazing incidence (15^0 above the horizon) is to extend the range about 100 meters, made up in the following way:

75 M	dry air
24 M	water vapor
1 M	condensed water.

The static values of these effects on the range measurement can be removed. The electrical range data, from the average of the values of range differences seen from the ground and from the satellite, will contain atmospheric fluctuations in the order of 0.3 meters (10 percent of the 3 meters of optical path) due to the atmosphere when measured at a zenith orientation. The fluctuations, being uncorrelated, will average out. Since ionospheric effects are small at .3 GHz., there should be little problem except for the fact that the ionosphere suffers 24-hour variations that may introduce a systematic bias to the range data.

The effect of the radial acceleration of the satellite due to the orbit eccentricity will produce a bias in the two-way averaged range data as determined aboard the satellite. The bias can be thought of as a variation in the time at which a certain value of range was computed. A correction for this can be made by calculating the necessary time (or phase) from a knowledge of the acceleration of the orbit as determined previously.

The measured relativistic frequency shift can now be compared to the predicted values determined from the orbit. This comparison will be made using data continuously obtained over the course of the experiment. The residuals from the best fit of the data will be analyzed to determine the nature of the "noise" that accompanies the data. From a knowledge of the "noise," a judgment can be made on how much data will be required to obtain the maximum accuracy from the experiment.

Certain internal checks are available on the performance of the apparatus. The frequency shift between apogee and perigee will give a measurement of the relativistic effect, and the accuracy of the measurement depends on the stability of the clocks. The time average of the satellite masers' frequency shift over a complete orbit compared to the ground masers' frequency will give a measurement of the relativistic effect that is limited by the precision of the clocks. These two methods of measurement should be consistent with each other within the limitation imposed by the precision of the clock.

The duration of the experiment will depend very much on what the data looks like after the initial 30 to 60 days running. It is important that some data reduction be done early in the experiment. The decision on whether to continue taking data will depend on the performance of the equipment, the importance of the additional data to the accuracy of the measurement, and on whether or not it is decided to search for other relativistic effects associated with the orbital motion of the earth about the sun.

2. Study of the Eccentric Orbit To Improve the Accuracy of the Experiment

The experiment as it is presently visualized consists of comparing, by electromagnetic signals, the rate of a clock in an orbiting satellite with that of a similar clock on the ground. The experiment would be performed using the following procedure. The two clocks are compared while both together on the ground, then one is orbited about the earth and compared with the ground clock via telemetry. By using an eccentric orbit one can, in effect, modulate the red shift. The average shift is the same as for a circular orbit and additional information is available from the modulation.

The expected effect, once the first-order doppler shifts in the telemetry are accounted for, is given by

$$\frac{\nu_s - \nu_e}{\nu_e} = -\frac{GM}{c^2}\left[\frac{1}{r_s} - \frac{1}{r_e}\right] - \frac{1}{2}\,\frac{v_s^2 - v_e^2}{c^2}$$

where ν_s is the satellite clock frequency

ν_e is the earth clock frequency

c is the velocity of light

GM is the gravitational constant of the sun

r_s is the satellite distance from the center of the earth

r_e is the radius of the earth

v_s is the satellite velocity

v_e is the earth station velocity due to rotation of the earth.

For a synchronous circular orbit the magnitude of $\frac{\nu_s - \nu_e}{\nu_e}$ is about 5.3 parts in 10^{10}.

This effect is measured with an accuracy that is limited by the precision of the satellite clock. Precision is the measure of the ability of the clock oscillator to be reset to its characteristic frequency. Currently the 1σ probability for this is 1 part in 10^{13} and consequently the accuracy of the measurement of the clock frequency is limited to about 2 parts in 10^4, or 0.02%.

By placing the clock in an elliptic orbit one enables the clock to scan a range of gravitational potentials in a periodic manner and a periodic comparison of the effect is possible with the ground clock. The important property of the clock for this

measurement is its stability. Fig. 12 (p. 24) shows the stability of a hydrogen maser as a function of observation time. The stability is defined here as the probability that a measurement of frequency averaged over time τ will be within one standard deviation of an average of frequency made over an adjacent interval of time τ. It is seen that experimental data in the $\tau = 10^2$-to-10^4 second region give stability values about one part in 10^{14}. If an eccentric 24-hour orbit is used it is reasonable to expect that frequency measurements can be made with this type of precision every 24 hours, and that a large number of data points can be accumulated. If there are no 24-hour spurious systematic variations in the clock operation, then the experiments can be treated statistically to give a mean value and a probable error of the mean value. This should improve even further the accuracy of the measurement of the effect.

By using an orbit with eccentricity e and semi-major axis, a, which is related to the 24-hour orbital period by $a = \left[\frac{\tau}{2\pi}\right]^{2/3}\left[GM\right]^{1/3}$, we obtain

$$\frac{\nu_s - \nu_e}{\nu_e} = \frac{GM}{c^2}\left[\frac{1}{r_e} + \frac{1}{2a}\right] + \frac{1}{2}\frac{v_e^2}{c^2} - \frac{2GM}{c^2}\frac{1 + \epsilon\cos\theta}{a(1-\epsilon^2)}$$

The first term has a magnitude of 7.5×10^{-10}.

The second term will be the same as for the circular orbit and depends on the latitude of the earth station.

The third term depends on the eccentricity and has maximum and minimum values, given in units of 10^{-10}, as follows:

ϵ	|Max.|	|Min.|	|Difference|
0	2.12	2.12	0
0.1	1.94	2.35	0.41
0.2	1.76	2.65	0.89
0.3	1.64	2.79	1.15
0.4	1.52	3.42	1.90
0.5	1.40	4.24	2.84
0.6	1.33	5.30	3.97
0.7	1.25	7.00	5.75
0.8	1.17	10.60	9.43

It is clear that the eccentricity will be limited by the requirement of keeping the satellite in sight of the ground station at all times. The maximum value of the angle of advance (or retard) of the satellite as observed from an equatorial station

is given in Figure 13. This is calculated for a $1/r^2$ force law; no effect due to higher order terms is included. For an eccentricity of 0.5, the satellite will remain visible from the ground and the maximum angle from the zenith will be about 68^0.

If we examine the relativistic frequency shift for this orbit as a function of angle, the following is found:

$$\frac{\nu_s - \nu_e}{\nu_e} - \frac{1}{2}\frac{\nu_e^2}{c^2} = 7.5 \times 10^{-10} - \frac{2.12 \times 10^{-10}}{.75} - \frac{2.12 \times 10^{-10}}{.75} \times 0.5 \cos\theta$$

$$= 4.67 \times 10^{-10} - 1.42 \times 10^{-10} \cos\theta$$

The constant term can be obtained by taking an average frequency shift over all angles that the radius vector of the satellite makes with respect to the stars, making the average value 4.67×10^{-10}. If a time average is taken, the result will be the same as for the circular orbit, i.e., 5.3×10^{-10}. This preserves the original aspect of the experiment since it makes use of the precision of the clocks.

Using such an elliptic orbit one should be able to measure a 2.84 parts in 10^{10} change in frequency every 12 hours, with a 1σ precision of one part in 10^{14}. This amounts to making a measurement of the effect with an accuracy of 3.52×10^{-5} every 24 hours. With a good accumulation of data, some very interesting statistics can be obtained. Furthermore, this orbit allows an internal check on the clock precision since the averaged data over 24 hours and the data obtained from 12-hour extrema should be consistent with each other.

It is clear that there will be a long list of effects that must be considered in detail in weighing the advantages and disadvantages of the eccentric orbit over the circular orbit. The following are a few examples.

The telemetry system will be required to cope with a wider range of first order doppler shift and operate over a wider range of angles from the zenith. Also, because of the wider range of "seeing" angle, better stationkeeping ability of the satellite will be required.

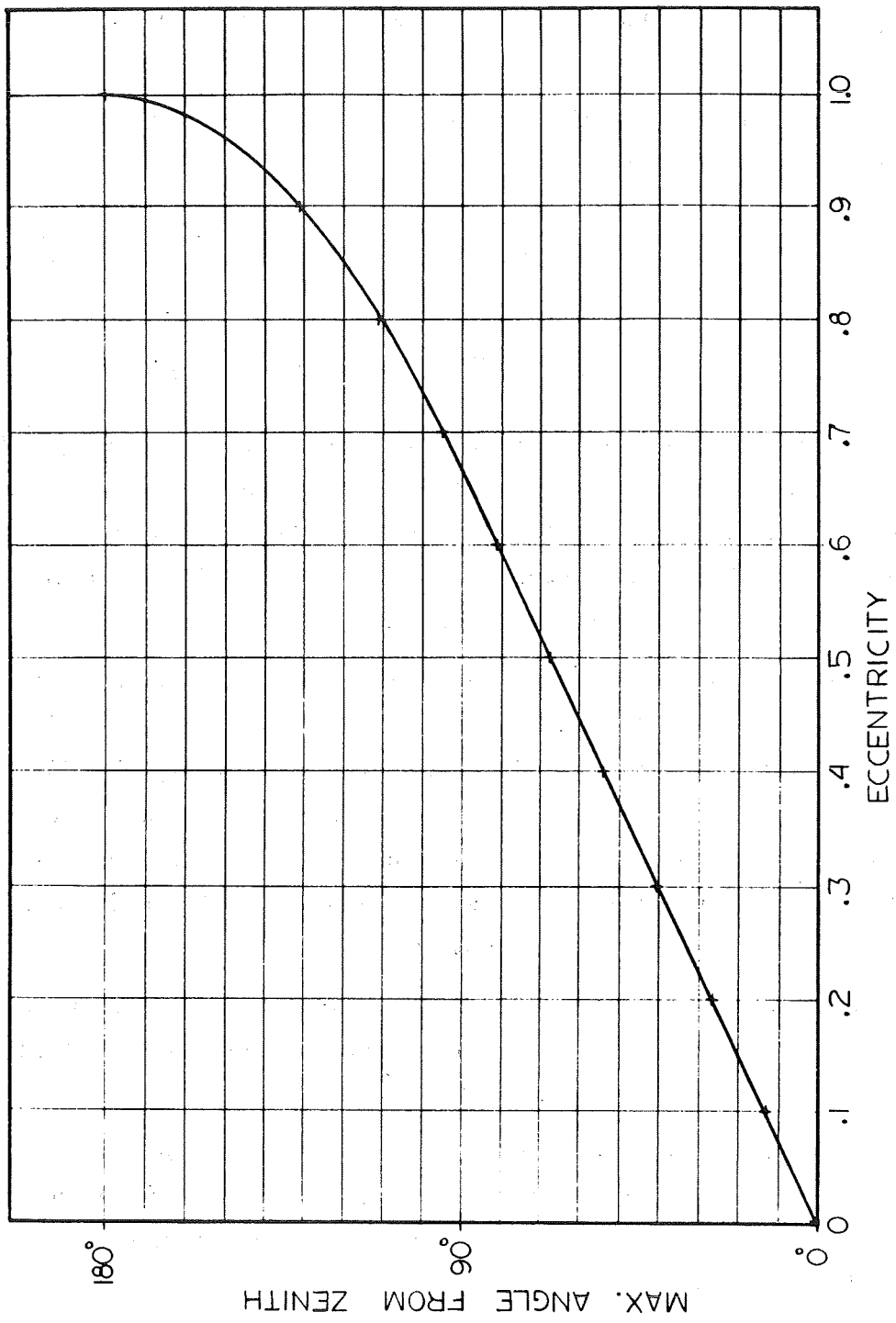

Figure 13.

The satellite will be exposed to radiation chiefly due to charged particles in the Van Allen belts. If any frequency shift occurs due to cumulative dosage, it will become apparent in the relative magnitude of the fixed and varying terms of the measured effect.

Gravity gradient stabilization of the orientation is likely to be more difficult or even impossible, depending on the eccentricity of the orbit.

Magnetic field variations with distance and orientation with respect to the earth dipole are small and are not likely to disturb the clock; however, great attention must be placed on all such position dependent effects since they have the same periodicity as the effect we seek to measure. An example of this is the reflected heat from the earth and its effect on the payload.

More payload may be possible with an eccentric orbit since the "apogee kick" is given at a lower altitude.

To make a more accurate comparison of the measured effect with predictions, correspondingly greater accuracy is required in the determination of the satellite velocity and position.

The improvement in accuracy of the measurement is likely to be about tenfold if an eccentric orbit is used.

The project development plan has been edited and places where the new orbit makes a difference to the plan have been identified. A more exact computer run involving orbits that are inclined eccentric orbits with various ground station locations has been done at M.I.T. and these data are presented in a paper shortly to be published in the Journal of Space Science and Applications,* which more thoroughly describes the theory of the experiment.

---

* "An Orbiting Clock Experiment To Determine the Gravitational Red Shift," by D. Kleppner, R.F.C. Vessot and N.F. Ramsey; to be published in the Journal of Astrophysics and Space Science.

III. OBJECTIVES OF CONTINUATION OF PROGRAM

The primary goal of the continuation of the program is to develop, build and test a self-contained hydrogen maser clock system that can be used in a satellite or as part of a ground system. Since specific environmental data on the particular type of vehicle to be used is not yet available, the mechanical interfaces and thermal guidelines described in the Project Development plan will be used. Acoustical and mechanical testing vibration levels as given in the Testing Plan will also be used.

The clock system consists of the following components, and reference is made to the experiment block diagram (Fig. 9, page 21) where the following items can be identified:

a. Two hydrogen maser oscillators.

b. Supporting electronics for the masers, thermal, pressure, diode, d.c. voltage, field currents, r.f. discharge.

c. Two phase lock systems and synthesizers.

d. Sequence timer and autotuner system.

e. Power supplies, telemetry signal conditioning, and command systems.

A. The Maser Oscillator

Effort in research or advanced development and engineering is required to accomplish the goal of performing a satellite clock experiment. The present state of the art in hydrogen masers permits comparison of frequency to be made to an accuracy of about one part in 10^{14} for adjacent samples 10^4 seconds in duration. This limitation is imposed by systematic effects that, in principle, can be controlled. As in many such situations, engineering improvements and more fundamental improvements can both be usefully pursued. In the case of the maser oscillator, the chief limitation is the pulling effect of the r.f. cavity resonance on the natural resonance of the hyperfine separation of the hydrogen atom. The magnitude of this effect is described by the expression

$$(\omega_o - \omega) = (\omega_o - \omega_c) \frac{Q_c}{Q_\ell}$$

where ω_o is the transition frequency of the hydrogen atoms in the maser bulb, ω is the output frequency and ω_c is the cavity resonance frequency. The quantity $\frac{Q_c}{Q_\ell}$ is the ratio of the loaded cavity Q to the line $Q = \frac{\omega}{\Delta\omega\ell}$ which depends on the unperturbed storage time of the atoms in the bulb.

The minimum cavity Q is determined by the filling factor of the bulb in the r.f. cavity (assuming no external r.f. gain is used), and the ratio of wanted to unwanted atoms obtained from the state selecting system. It is seen that the pulling effect depends on the product of the mistuning $(\omega_o - \omega_c)$, and the linewidth of atomic hydrogen transition, $\Delta\omega_\ell$. By better cavity design, the use of the latest ultra-low expansion materials such as Corning's ULE Quartz or Owens-Illinois' Cer-Vit, and thermal control, the mistuning effect can be reduced by at least a factor of ten. The natural linewidth, $\Delta\omega_\ell$, depends on the ability to store atoms in an unperturbed manner in the bulb of the maser. At present the chief limitation is the probability of recombination of atoms when they hit the wall of the bulb. It is proposed that continued effort in engineering and research be done to improve further the performance of the maser oscillator beyond the one part in 10^{14} that is the current state of the art.

Present coatings have all been of Teflon--either the TFE homopolymer or the FEP copolymer--applied from water dispersions. Other methods of applying Teflon such as polymerization in the bulb from the gas phase will be tried. Coatings of other fluorine polymers will also be tried. It should be remembered that any advantage in storage time obtained will result directly in a comparable improvement in maser stability.

Work on improvements in mechanical and thermal design will be continued. Total weight of the maser oscillator system with its supporting electronics, receiver and synthesizer can be reduced considerably. A reasonable goal at present is to get the package down to less than 300 lbs. Of this weight some 250 lbs. will be in the maser oscillator. Mechanical testing of the various components will be continued and these assemblies will be used as design inputs for a new design.

A lightweight and compact gas handling system will be developed based on the presently used designs. Since it has been found possible to control the

atomic hydrogen flux into the bulb by adjusting the degree of r.f. excitation in the dissociator, fast pressure variations in the discharge are no longer required and the design of the palladium valve pressure control can be simplified.

B. Supporting Electronics

Thermal control of the maser is provided at several levels and depends very much on the environment to be expected. The present status of this work is to consider a 30 ± 10°C external ambient that may well be the result of an external temperature control system. The power dissipation of the active elements, i.e. the pump and discharge, will not exceed 20 watts, and it is likely that about 25 watts of heating power are required to keep the maser under thermal control when the external ambient drops to 20°C. It is assumed that the external system will provide a heat sink for this power while maintaining the above temperature limits.

Control of temperature is maintained at three places: two levels of thermal control about the cavity and a thermal guard station at the neck. Temperature is sensed by glass bead thermistors in a bridge circuit whose output is led to an operational amplifier. This circuit is located within the temperature controlled region and its output is led to the efficient power controller using the pulse duration mode of control.

Hydrogen pressure to the discharge is controlled by adjusting the permeation rate of hydrogen from a bottle at about 1000 psi through a palladium silver pellet. The rate of permeation depends on the temperature of the pellet. The molecular hydrogen in the line feeding the dissociator is in the 0.01 to .1 mm Hg pressure range and is sensed by a thermistor pirani gauge. The thermistor is self-heated by an electric current that is servoed to keep the thermistor at a constant resistance. Since the power required to maintain the constant resistance depends on the cooling effect of the hydrogen, the thermistor current is a sensitive indication of pressure and is used to control a power amplifier that provides power to heat the palladium pellet. In this way the pressure is servo controlled to a given preset level. As mentioned in the previous section, fast changes of pressure are not required and the rate of heating and cooling of the palladium

can be slow, allowing more efficient use of power to heat the palladium. The low level circuitry has been developed and the power handling can be done efficiently using a pulse-duration control similar to that used for the maser temperature controllers.

D.C. power to the r.f. exciter is also controlled using pulse-duration (or switching) type controllers. Changes in excitation from "high" to "low" are made automatically by the autotuner; the levels are preset using a potentiometer.

C. The Phase Lock System

In this system the low level, high stability and high spectral purity signal from the maser is used to control a crystal oscillator. A double superheterodyne receiver is used with a low noise diode mixer at the input. The first I.F. frequency is 20.4 MHz and the gain of the first stage is about 25 db. A second mixer converts the frequency to 405 kHz and this stage has about 90 db gain. The first local oscillator signal is at 1400 MHz and is multiplied from a 100 MHz crystal oscillator (or a 5 MHz oscillator, which is more reasonable since this crystal oscillator will then be of the highest available stability and can be used as a tuning reference in the event of a maser failure). The second local oscillator signal is at 20 MHz and is derived from the crystal oscillator.

The output signal at 405 kHz is compared in phase with a signal of the same frequency synthesized from the crystal oscillator. The output from the phase detector is led to an operational integrator. This signal is led to the variable capacitor in the crystal oscillator and corrects the phase of the oscillator so that there is a constant ratio of crystal frequency to maser frequency. The operational integrator in the operational amplifier minimizes the static phase error in the systems.

D. Timing System and Autotuner

The feasibility of using an automatic system for adjusting the cavity resonance to the frequency determined by the radiating atoms in the maser bulb was first established under contracts NAS5-11598 and NASW-1337. In these tests,

commercially available bi-directonal counters were used to count streams of pulses that were gated by a preset number of zero crossings in the beat frequency between two masers. The number of these gated pulses is directly related to the period of the beat. By counting in one direction, say upward, at high source pressure and in the downward direction at low source pressure, the effect of quenching due to high pressure spin interaction between atoms in the bulb can be detected as a frequency shift, the magnitude and sign depending on the cavity mistuning. Thus, any residual count on the register after a high and low pressure run is a direct measure of the mistuning. This count, converted to a d.c. voltage at the cavity varactor diode, can be used to correct the cavity frequency.

A binary counting system, jam transfer system and digital-to-analog system has been constructed using integrated circuit components and will be tested. A frequency divider system will be designed so as to operate a clock system and an automatic sequencer for the autotuner. The presently used breadboard timer has a great deal of flexibility for setting up various time cycles and will be used to determine optimum counting periods and cycling rates. The timer will then be redesigned using NASA-approved types of components and packaged with the present binary autotuner.

With minor changes in counting period and averaging time, the same counter can be used for tuning the maser with a crystal oscillator as reference. The design will also include this mode of operation.

E. Power Supplies, Telemetry Signal Conditioning and Command Systems

It is proposed that the signal conditioning equipment for the telemetry be developed at a later date; however, signals from the places that must be monitored will be made available at suitable levels and suitably isolated electrically for input to a telemetry system. This system is not, as yet, specified, and will be developed to accommodate the requirements of the mission when the mission is defined.

In the case of telemetered voltage, current and switch position or logic information, the approach will be to employ manual adjustments that, at a later

time, can be replaced by digitally operated systems. In places such as the autotuner that is already a digital device, the information to the autotuner (e.g., a setting of a tuning diode) will be provided in digital form.

Power supplies for operating the clock system while under test will be commercially obtained. The development of suitable supplies for the satellite as a whole will be deferred until more information is available. Precision supplies for the varactor diode voltage and for the magnetic field controls will also be adapted from commercially available equipment.

Work on the commanded degausser and the commanded low frequency system for magnetic field measurement will be deferred until more fully developed flight hardware plans are made.

IV. CONCLUSION

The subject contract has been interrupted and the work has not been completed. Further mechanical testing and thermal testing remains to be done. Electronic testing of the thermal controller breadboard and of the binary logic form of the autotuner also remains to be done.

The program involving the satellite maser and its subsystems has been transferred to the Smithsonian Astrophysical Observatory in Cambridge, Massachusetts, and work in the directions described in Section III will proceed and will be coordinated into a program involving measurements of angular diameters of radio sources by long baseline interferometer techniques. Measurements of continental drift and measurements of relativistic light (or radio wave) deflection by massive bodies such as the sun are also planned using the maser clock developed under the program. The same type of apparatus also lends itself to performing time synchronization at distant points on the globe.

The satellite clock experiment to verify the principle of equivalence continues to be studied, and its importance is not diminished. The present period of reorganization within the Government, redeployment within NASA, and relocation of the principal investigation for this experiment has delayed for a time the performance of the experiment; however, it is to be hoped that the very fundamental measurement now possible with the maser clock, by placing it in orbit and measuring the difference between the time scales as originally contemplated, will eventually be performed. As the space program evolves and as deeper and deeper excursions are made toward the planets of the solar system, and even beyond the solar system, the satellite clock will become increasingly important to the success of these missions.

V. NEW TECHNOLOGY

Two items of new technology are reportable for this phase of the program. The first is the method of cavity support using syntactic foam as described on pages 15 and 17 of this report. The second is the self-jigging stacked array mount for the hydrogen atom source. This is described on page 13 and shown in Figure 6 of this report.

APPENDIX I

DATA REPORT OF INITIAL VIBRATION TESTING OF R&D HYDROGEN MASER

by

VIBRATION AND ACOUSTICS BRANCH
STRUCTURES DIVISION
PROPULSION AND VEHICLE ENGINEERING LABORATORY

N.A.S.A. - MARSHALL SPACE FLIGHT CENTER
Huntsville, Alabama

August 1968

TABLE OF CONTENTS

I. INTRODUCTION

A critical part of the Phase I Developmental Program of the Redshift Relativity Experiment involves the production of a Hydrogen Maser to the point of demonstrating compatibility of the Maser design to the launch vehicle environments. To accomplish this purpose, three significant objectives were defined:

(1) To subject the "breadboard" Maser System to vibration excitation over a wide range of frequencies and amplitudes, covering the approximate range of environments which might be encountered in the launch vehicle payload areas.

(2) To measure significant operational functions and parameters during environmental exposures, which would identify any deterioration, malfunction, or failure of the system which might be corrected by redesign.

(3) To measure the major structural and mechanical responses within the test item in order to define mode shapes, response frequencies, and stress levels.

This data report is directed toward the presentation of the test procedures, test results, data acquired, and basic design problems encountered during the initial vibration testing of the R&D Hydrogen Maser.

All vibration testing of the Maser was completed using sinusoidal forcing functions. Random environment testing was originally scheduled, but was cancelled due to the lack of recording and data reduction equipment.

II. SUMMARY

Due to a lack of recording equipment, the majority of the vertical axis test data was obtained from voltmeter readings. The lateral axis test data, however, was acquired with the use of a modified 8-channel strip chart recorder.

In light of the limited recording ability, the data must be viewed objectively. It should be used only as an indication of the response frequencies and the structural transmissibilities.

Quantitatively, the data shows that the present design of the R&D Hydrogen Maser is adequate for the environmental vibration levels to which it has been subjected. Some design changes were deemed necessary due to vibration testing, and will be incorporated before the next phase of testing.

Enclosures I and II contain instrumentation plans and tabulated response data for the vertical and lateral axes tests, respectively.

III. GENERAL

The vibration tests were rigid interface tests, with the test package mounted at representative attachment points to a rigid fixture which was in turn attached to a vibration exciter. Tests were performed in two orthogonal axes, one of which was parallel to proposed vehicle flight axis.

Sinusoidal sweep tests as specified in tables I and II were performed, starting at the lowest specified levels and progressing through the highest in each axis. A thorough data evaluation was accomplished after each test to identify any deterioration of performance or response. Test levels and frequencies at which adverse effects appeared were noted as closely as possible.

The vertical axis test setup and equipment was considered adequate for performing a sinusoidal test on the Maser System, with the exception of the lack of recording equipment. This test series was conducted at Bomac Laboratory. The lateral axis setup at Bomac Laboratory was evaluated, and termed undesirable for that portion of the Maser testing.

The lateral axis test was completed at Lincoln Laboratory, Bedford, Massachusetts. Although an acceptable lateral axis vibration test was accomplished, the equipment existing at this laboratory is objectionable in its present state. The shaker system contains equipment ground loop problems and equipment calibration problems, which required more working time than did the actual testing. In general, some additional maintenance and system checkout should be required before further testing is scheduled in this laboratory.

IV VERTICAL AXIS VIBRATION TESTING

Table I contains the environmental test requirements imposed on the Maser in the vertical axis at Bomac Laboratory, Beverly, Massachusetts.

Table I. Developmental Test Requirements (1 oct/min.)

Phase A:	5 - 16 cps @ 0.075 in. D.A. 16 - 2000 cps @ 1 g peak
Phase B:	5 - 16 cps @ 0.15 in. D.A. 16 - 2000 cps @ 2 g's peak
Phase C:	5 - 16 cps @ 0.3 in. D.A. 16 - 2000 cps @ 4 g's peak

The following is a brief account of the test procedure, problems, solutions, and results obtained during the vertical axis testing of the R&D Hydrogen Maser.

1. A Phase A vibration test level was performed first on the Maser. The sine sweep was well controlled and no response problems were encountered.

2. A Phase B test was then accomplished. During this test, many random chattering resonances were noticed. These were believed to be emanated from the silica cavity cylinder and bottom cavity plate interface. To solve this chattering problem the wall and bottom plate were fastened together with epoxy cement.

3. At this point, the Maser was retested at the Phase A and Phase B levels. Recorded data was satisfactory with no hazardous levels being evident.

4. With all previous accelerometer data yielding no detrimental responses, Phase C testing was initiated. A distinct change in the audible sound and response frequency of the cavity was noticed during the Phase C testing. It was then decided to perform an inspection of the test article.

5. Results of the inspection were :

(a) Accelerometer # 3, which was located over a suspected structurally deficient expansion leg area, debonded during the test.

(b) A large crack was found in the bottom silica cavity plate. The crack had propagated from the suspect leg area to the center hole in the silica plate.

(c) A maximum of about 30 g's at 900 cps at accelerometer # 5 (which is similar to # 3) was noted during the Phase C test.

(d) It was surmized that the failure was a localized one, due to the nature of the propagation, and could be corrected with a minor design change.

6. A new silica cavity bottom plate was obtained, and after inspection, appeared to be in good condition. To help eliminate some of the localized stresses, soft copper washers were placed under the expansion legs. At this point an 8-channel strip chart recorder was also installed for use on four response accelerometer locations. Up to this time, all data had been recorded with the use of voltmeters.

7. In order to check the calibration and operation of the recorder, a Phase A test level was run.

Accelerometers # 3, # 8, # 11, and # 12 were connected to the recorder and monitored during the Phase C testing.

Again an inspection was performed on the Maser. Results of this inspection revealed no structural damage.

8. A fixture evaluation was run on the lateral axis setup at Bomac Laboratory before placing the Maser in the system. The vibration linkage between the fixture and shaker decoupled and proved to be undesirable above 400 cps.

The lateral axis testing was then scheduled to be run at Lincoln Laboratory, Bedford, Massachusetts.

V. LATERAL AXIS VIBRATION TESTING

Table II contains the environmental test requirements for the Maser in the Lateral axis at Lincoln Laboratory, Bedford, Massachusetts.

Table II. Developmental Test Requirements (1 oct/min.)

Phase A:	5 - 16 cps	@ 0.04 in. D.A.
	16 - 2000 cps	@ 0.5 g peak
Phase B:	5 - 16 cps	@ 0.15 in. D.A.
	16 - 2000 cps	@ 2 g's peak
Phase C:	5 - 16 cps	@ 0.3 in. D.A.
	16 - 2000 cps	@ 4 g's peak

The following is a summary of the test procedure, problems, solutions, and results obtained during the lateral axis testing of the R&D Hydrogen Maser.

1. A fixture evaluation on the lateral axis setup was accomplished, and results proved the fixture to be adequate for the Maser testing.

2. Two Phase A test levels were then run on the Maser in order to determine which 8 accelerometers of the total 15 would be recorded during subsequent tests.

3. Phase B levels were completed with accelerometers # 1, # 2, # 5, # 6, # 7, #9, # 11, and # 12 connected to the strip chart recorder. A close analysis of the data was then begun before going to the Phase C test level.

4. The entire cavity was found to have a resonance below 200 cps. This low frequency resonance also affected the control ability of the shaker system. To alter this resonance, it was proposed to increase the preload on the spring loading mechanism. The adjustment screw torque was increased from about 10 in-lb. to 20 in-lb.

5. A Phase B test level was again conducted, with excellent control and good resulting data. The resonance was shifted and damped, and input control was adequately maintained across the entire frequency band.

6. With the completion of the first two environmental levels and the discovery of no other pronounced low frequency resonances, Phase C testing was initiated.

7. Inspection of the Hydrogen Maser after all testing was completed, revealed no structural damage to the system.

VI. CONCLUSIONS

The basic conclusions that can be drawn from these preliminary tests on the R&D Hydrogen Maser are:

1. The vertical and lateral axes testing data obtained thus far tends to indicate that Maser design is compatible with the sinusoidal vibration environments to which it has been subjected.

2. Three design changes were deemed necessary from this testing:

(a) The cylindrical cavity is to be fastened to the cavity bottom plate with epoxy.

(b) The expansion legs should be isolated with soft copper washers.

(c) The "Bootstrap" system, which constitutes the stability of the unit, must be stiffened, or pretension loads should be increased.

3. All major vertical and lateral axes resonances are in the higher frequency domain (> 200 cps).

ENCLOSURE I

VERTICAL AXIS VIBRATION DATA

ACCELEROMETER LOCATIONS

(Vertical Axis)

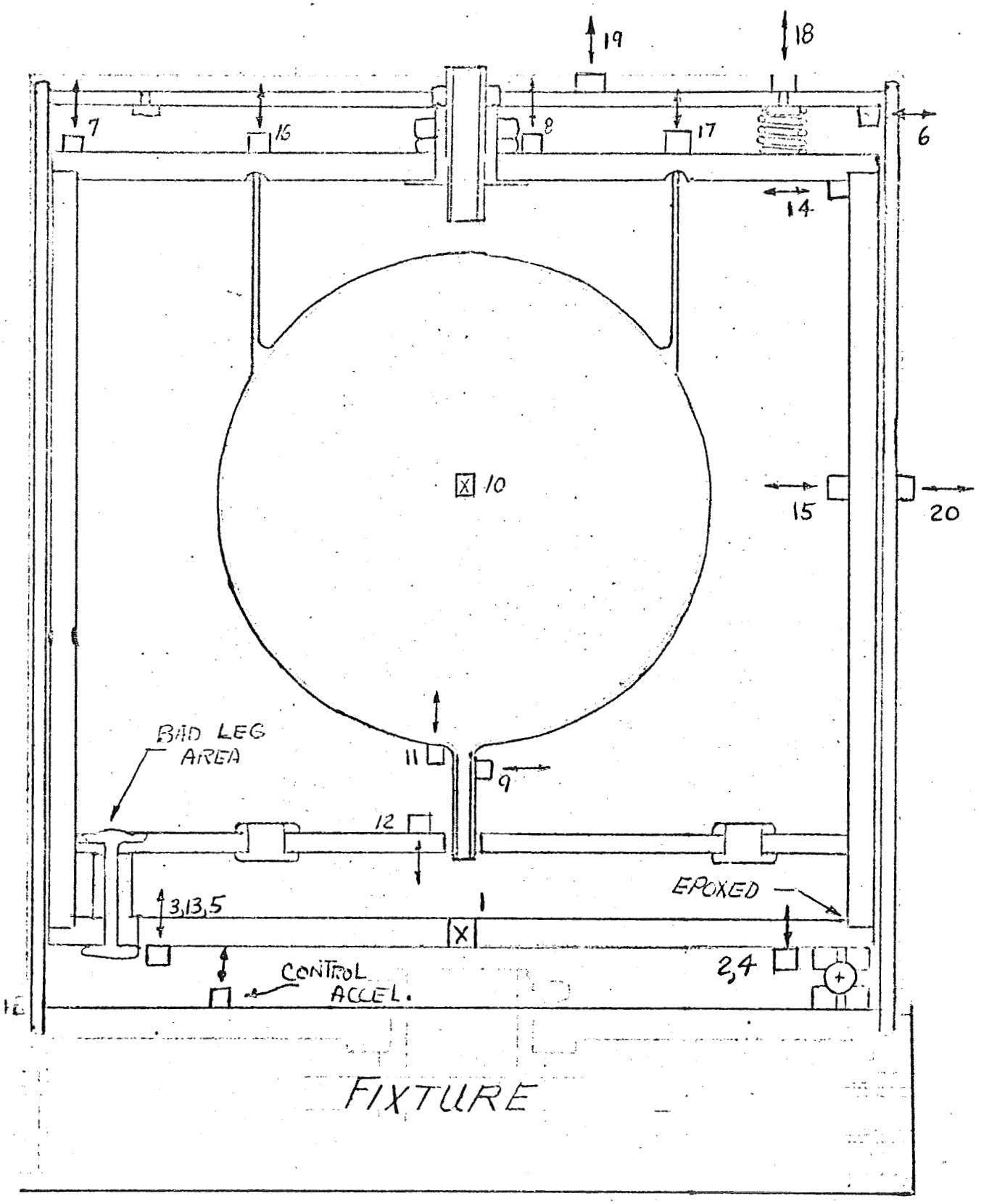

FIGURE 1

RUN I: PHASE A (Vertical Axis)

	ACCELEROMETER	FREQUENCY	G LEVEL
ZONE 1	# 3	260 cps	*
	#11	340 cps	21 g's
ZONE 2	# 8	460 cps	10 g's
	#18	550 cps	20 g's
ZONE 3	# 8	940 cps	18 g's
	#3, 12	940 cps	*
	#18		

RUN 2: PHASE A (Vertical Axis)

ZONE 2	# 9	430 cps	10 g's
	# 7, 8, 11, 12	460 cps	*
	# 9	480 cps	6 g's
	# 9	700 cps	9 g's
	#12	900 cps	120 g's
	# 9	1100 cps	11 g's
ZONE 3	# 7, 8	1100 cps	18 g's
	#19	1100 cps	18 g's
	#10	1100 cps	10 g's
	# 9	1250 cps	10 g's

RUN 3: PHASE B (Vertical Axis)

ZONE 2	#11	480 cps	18 g's
	# 7, 12	480 cps	*
ZONE 3	# 7, 12	760 cps	*
	# 9	900 cps	24 g's
	#11	900 cps	25 g's

RUN 4: PHASE C (Vertical Axis)

	ACCELEROMETER	FREQUENCY	G LEVEL
ZONE 1	#11	90 cps	6 g's
	#11	210 cps	6 g's
ZONE 2	# 9	480 cps	7100 g's
	#11	480 cps	7100 g's
	#12	480 cps	100 g's
	# 8	480 cps	24 g's
	# 7	480 cps	*
ZONE 3	# 5	900 cps	30 g's
	# 9	900 cps	60 g's
	#12	900 cps	100 g's
	# 9	1250 cps	60 g's

RUN 5: PHASE C (Vertical Axis)

ZONE 1	# 8	230 cps	12 g's
	#12	230 cps	13 g's
	#11	230 cps	8 g's
	# 3	340 cps	15 g's
+			
ZONE 2	# 8	400 - 500 cps	150 g's max
	#12	400 - 500 cps	110 g's max
	#11	400 - 500 cps	150 g's max
	# 3	400 - 500 cps	100 g's max
+			
ZONE 3	# 8	750 - 1250 cps	110 g's max
	#12	750 - 1250 cps	200 g's max
	#11	750 - 1250 cps	115 g's max
	# 3	750 - 1250 cps	110 g's max

* Significant response either not recorded or undercalibrated.

\+ Broadband of Resonances.

ENCLOSURE II

LATERAL AXIS VIBRATION DATA

ACCELEROMETER LOCATIONS

(Lateral Axis)

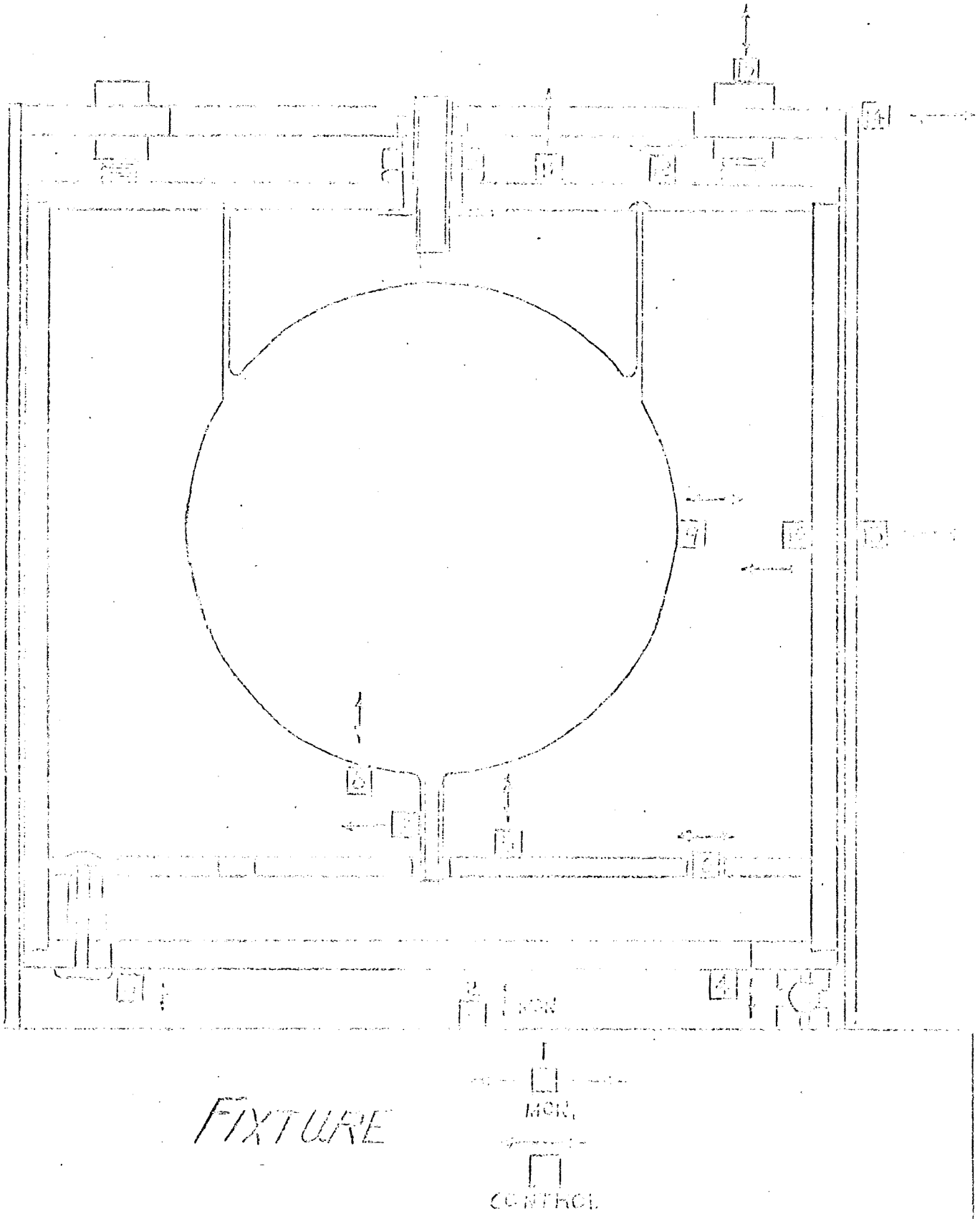

FIGURE 2

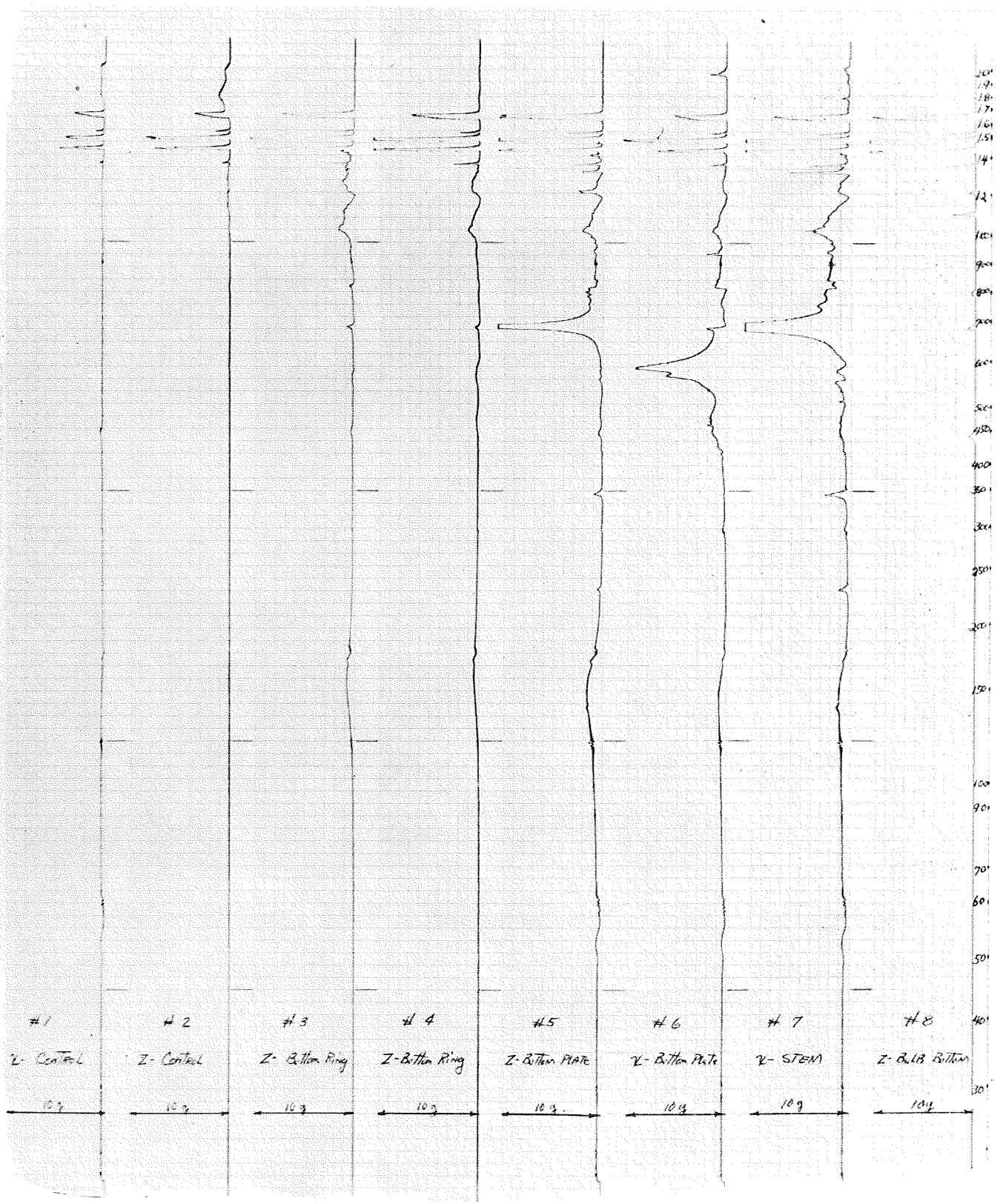
#1
Z- Control
10 g
#2
Z- Control
10 g
#3
Z- Bottom Ring
10 g
#4
Z-Bottom Ring
10 g
#5
Z-Bottom PLATE
10 g
#6
X- Bottom Plate
10 g
#7
X- STEM
10 g
#8
Z- BULB Bottom
10 g

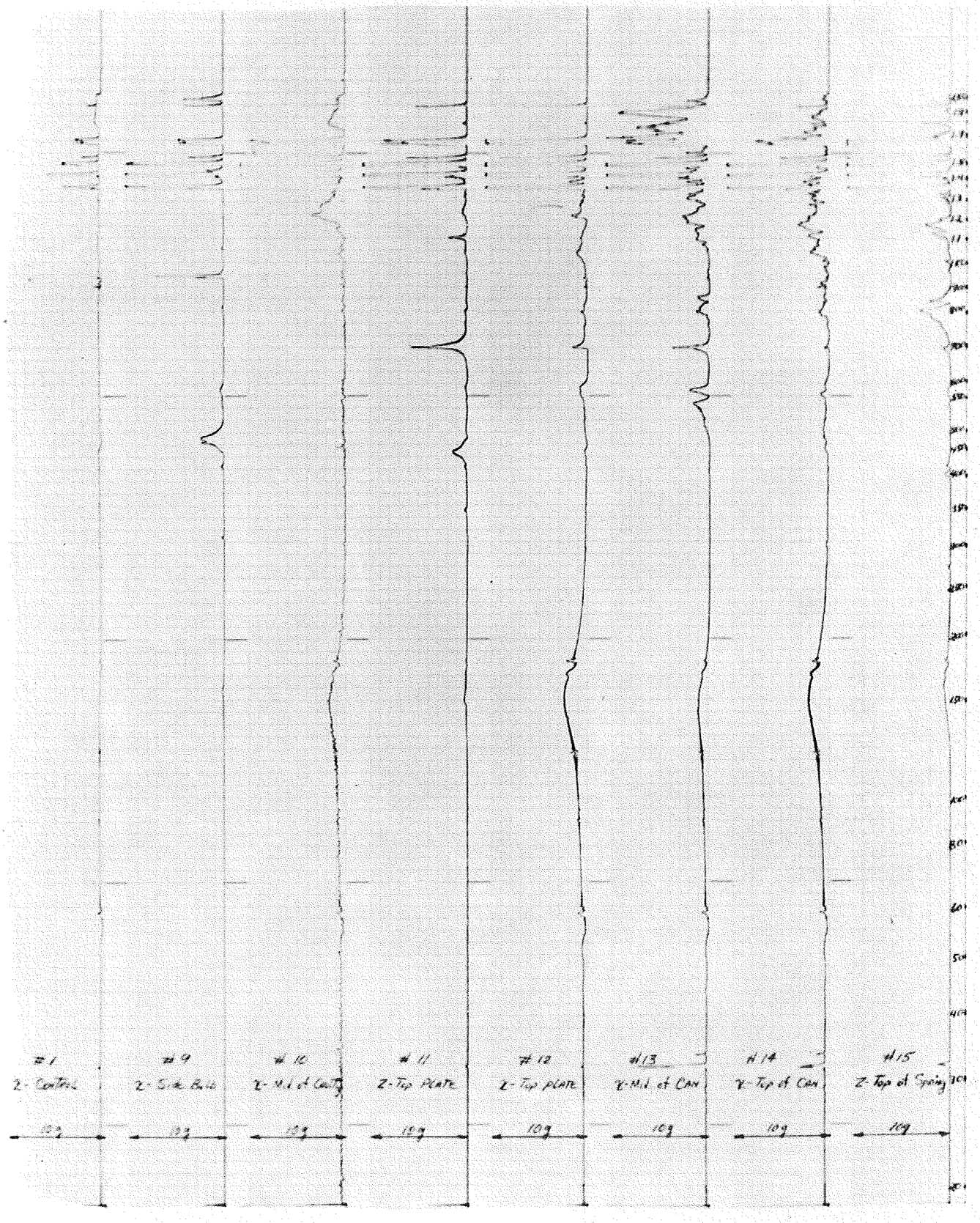
#1
Z- Control
10g
#9
Z- Side Rail
10g
#10
Z- Mid of Can
10g
#11
Z- Top Plate
10g
#12
Z- Top Plate
10g
#13
Z- Mid of Can
10g
#14
Z- Top of Can
10g
#15
Z- Top of Spring
10g

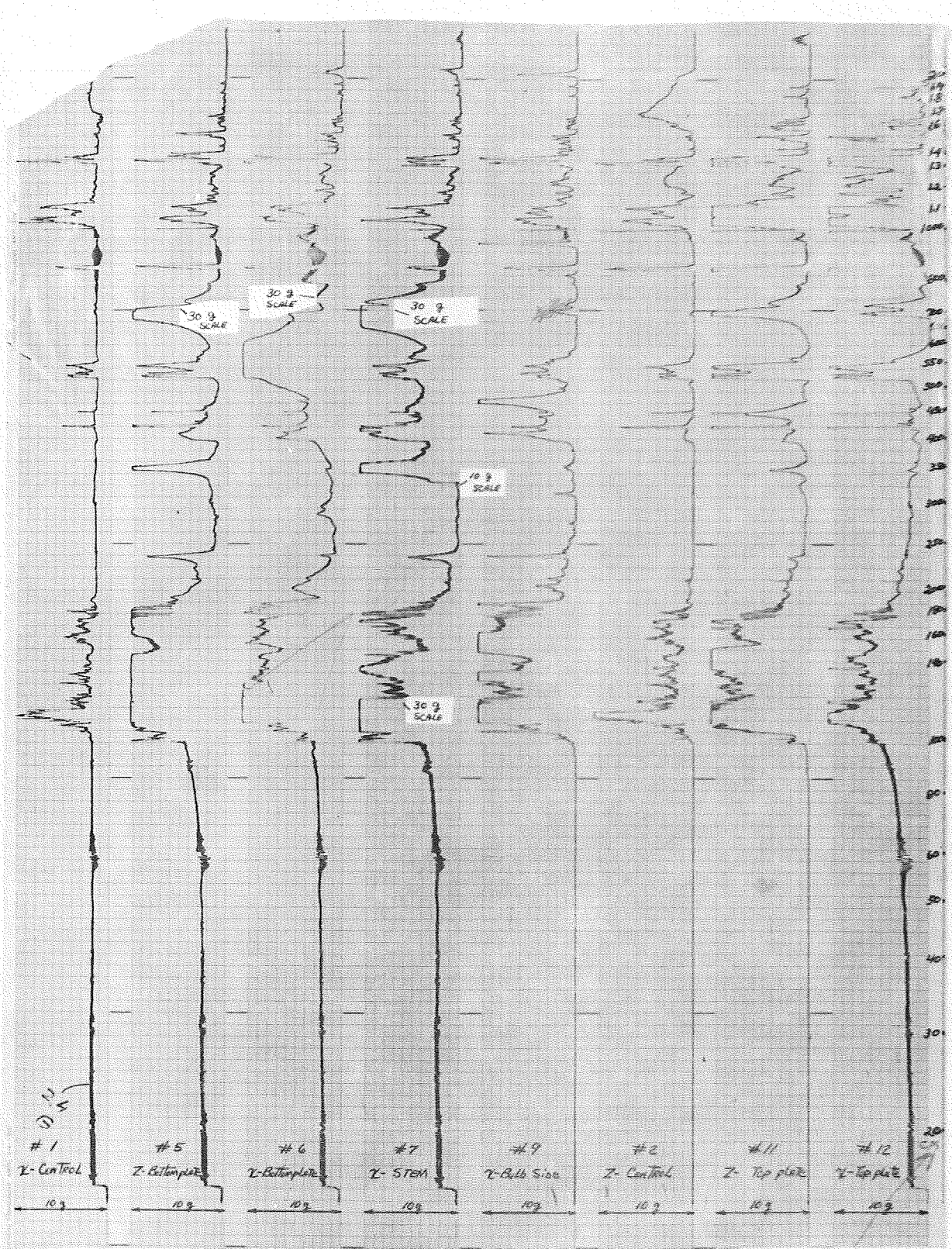

PHASE B TEST LEVEL

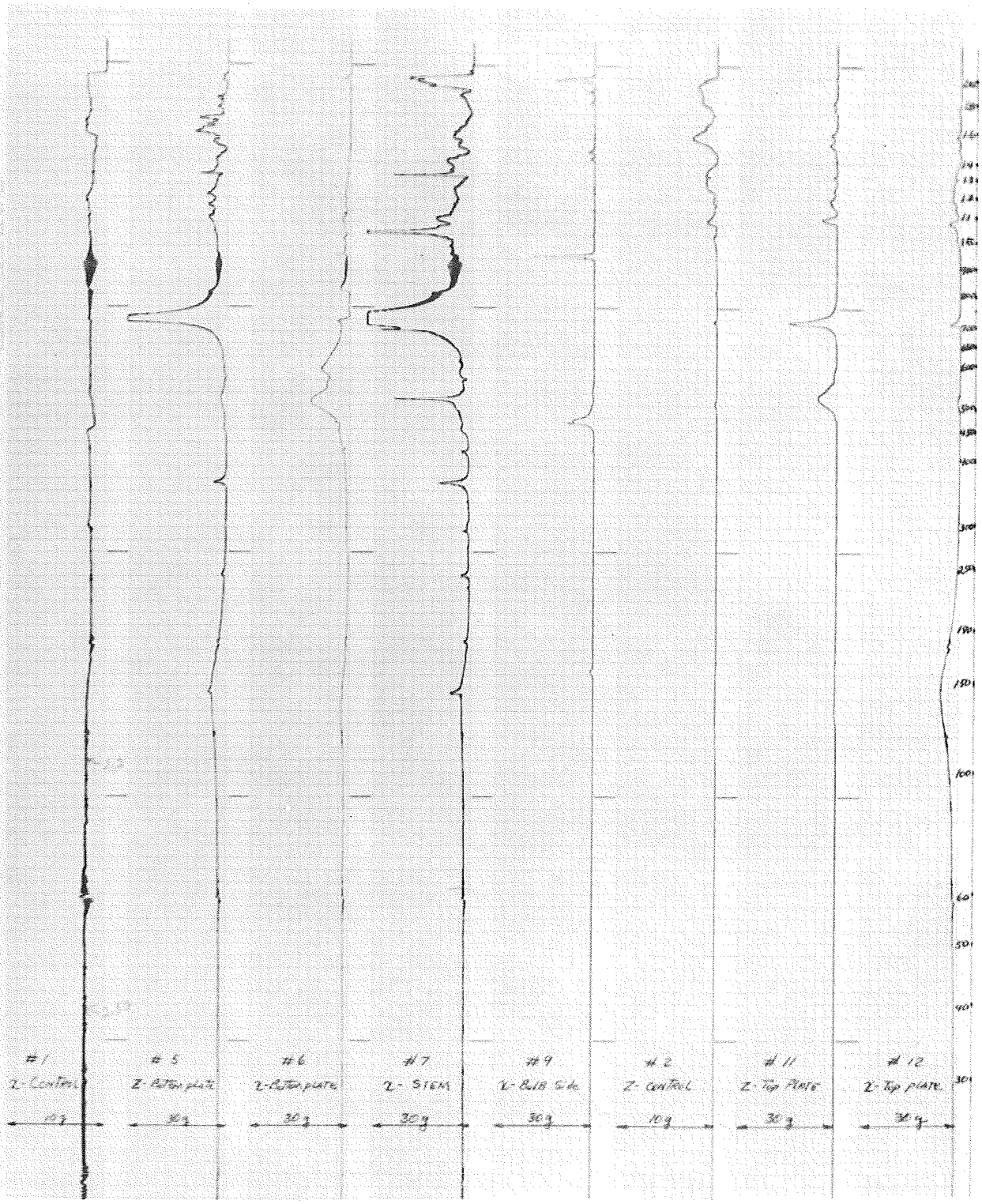
#1
Z- Control
10 g
#5
Z- Piston plate
30 g
#6
Z- Piston plate
30 g
#7
Z- STEM
30 g
#9
Z- Bulb Side
30 g
#2
Z- Control
10 g
#11
Z- Top Plate
30 g
#12
Z- Top plate
30 g

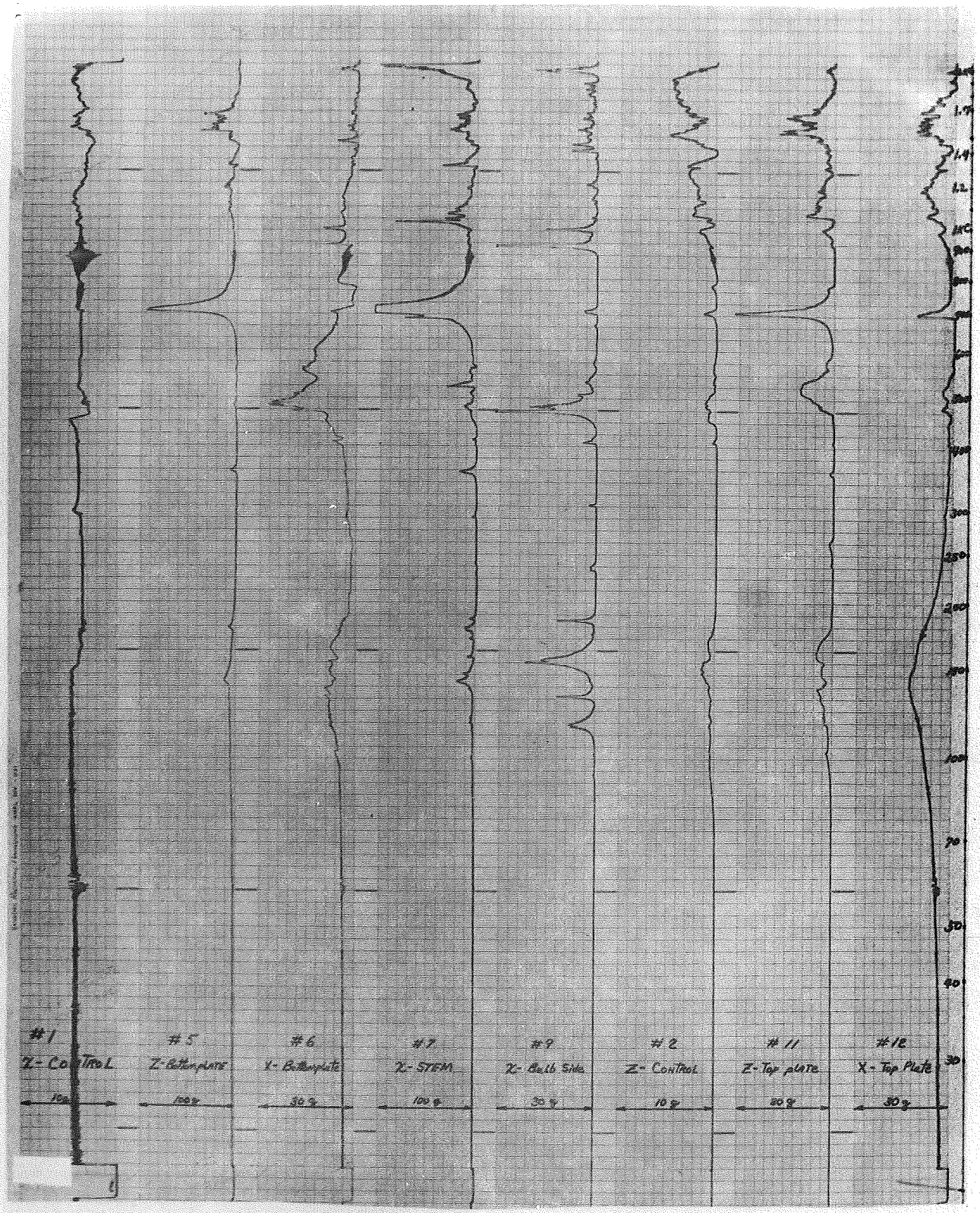

PHASE C TEST LEVEL
LOAD SPECIES PLANNED
20 m-kg on all SURFACES

SATELLITE MASER EXPERIMENT S-081 OPERATION PLAN

1.0 Pre-Launch Check-Out Procedures

A visual check will be made of the mechanical integrity of the assembly prior to final enclosure in the payload compartment of the vehicle. The position of all test switches, the removal of all test cables, and temporary equipment will be verified. The check-out and final calibration will be made through the command and telemetry equipment wherever possible either through the antenna system or via cables that bypass the r.f. portions of the telemetry system.

1.1 Maser operating systems.

a) Temperature control;
b) Pressure control;
c) Dissociator -- color;
d) Vacuum chamber pressure.

1.2 Maser oscillation check.

a) Signal levels versus source pressure;
b) Zeeman frequency versus applied C-field current;
c) Cavity tuning system.

1.3 Maser signal conversion systems.

a) Phase lock system lock range and noise;
b) Phase lock seek and hold system;
c) Maser self-tuning system;
d) Signal processing and frequency converters to telemetry system.

1.4 Command systems.

a) Autotune over-rule system;
b) Pressure command system to all masers;
c) Diode voltage command system (all masers);
d) Zeeman sweep system.

1.5 Maser system telemetry.

a) Beat between masers;
b) Signal strength of each maser;
c) Source pressure of each maser;
d) Manifold hydrogen pressure of each maser;
e) Maser cavity temperature of each maser.

1.6 Final comparison of pair of satellite masers with those on the ground.

a) Assuming all the previous systems are working, then set the self-tuning system and record the frequency relationship between all masers.

b) Measure temperature of all maser bulbs;
c) Measure all Zeeman frequencies;
d) Obtain a reasonably long record of maser beats to check system long-term performance.

2.0 Pre-Launch Status

Ground system equipment is functioning and experiment recorders are on standby. Range transponder recorder is on standby.

2.1 Hydrogen pressure and r.f. excitation levels set.

2.2 Satellite maser hydrogen off.

2.3 Discharge off.

2.4 Thermal controls on.

2.5 Maser signal processing electronics off.

2.6 Magnetic fields off.

2.7 Autotune D.A. switches set in most recent, best tuned position.

2.8 Ratio transponder ON (part of Doppler cancelling system).

2.9 Logic switches in automatic mode.

2.10 VacIons off unless long delays (weeks) are anticipated.

2.11 Housekeeping telemetry system off.

3.0 Launch Phase

Quiet meditation.

4.0 Parking Orbit Status

As in Pre-Launch Status except turn on VacIon pumps.

5.0 Final Orbit Status

At this point the outer casing has been jettisoned, the satellite is oriented, the solar panels are deployed, primary power is available.

At some time during this phase a range reading will be obtained from the guidance and tracking system. Differences from this reading will be read from the ratio transponder of the Doppler tracking system and be used for subsequent range information.

6.0 Checkout of Satellite Maser Clock System in Orbit

6.1 Experiment command system turned on.

6.2 Experiment telemetry system turned on.

6.3 Ground equipment recorders for housekeeping telemetry turned on.

6.4 Check VacIon current and voltage.

6.5 Check voltage on primary power.

6.6 Turn on maser signal processing electronics and maser support electronics that have been turned off.

6.7 Check primary power system voltage and current.

6.8 Check regulated supply voltages and current.

6.9 Check all thermal control current:

a) Inner oven;
b) Center ovens;
c) Casing;
d) Crystal ovens.

6.10 Check temperature at all monitored positions.

6.11 Check binary status of D.A. voltage to varactor.

6.12 Check source pressure.

6.13 Check synthesizer system:

a) 100 MHz crystal oscillator level;
b) 1400 MHz level;
c) 20 MHz level;
d) 400 kc level and frequency;
e) 400.080 kc level and frequency.

6.14 Turn on field controls.

6.15 Check field currents.

6.16 Turn on hydrogen.

6.17 Check hydrogen pressure.

6.18 Check VacIon current.

6.19 Turn on r.f. discharge.

6.20 Check color of discharge.

6.21 Look for maser signal:

a) Check second I.F. amplifier signal level;
b) Check phase detector output;

6.22 Start phase lock acquisition system:

a) Check phase detector output;
b) Check static phase error.

6.23 If, at this point, a maser is not oscillating, the following adjustments should be made by command:

a) Vary source pressure.
b) Set magnetic fields to high field.
c) Sweep the varactor voltage slowly over full range.
d) Degauss maser and repeat (a), (b) and (c). The degaussing cycle is as follows:

1. Turn off current to magnetic field coils.
2. Command high current contactor to connect to bell jar.
3. Select level of degauss current.
4. Apply degaussing current.
5. Remove high current contactor.
6. Check inner oven and bell jar temperature.
7. Check inner oven and bell jar heater current.
8. Repeat at lower level if necessary.
9. Final degauss cycle should be done with field current at normal operating values.

e) When maser operates, adjust field current to low field operation.

6.24 Measure low frequency transitions of all masers:

a) Raise flux to get a high level of oscillation.
b) Transmit frequency via telemetry using manual or automatic sweep.
c) Command level of signal to "Zeeman" coils.
d) Monitor signal level of second I. F. amplifier.

6.25 A maser that requires a gross readjustment of field should be degaussed prior to adjusting trim current for highest level of output at reduced flux.

a) Reduce flux either by pressure or excitation level.
b) Check threshold.
c) Set pressure or excitation slightly above threshold.
d) Adjust trim coil current for best output.

6.26 Remeasure field.

6.27 Readjust field coil current to obtain average 1 $m\ddot{0}$ level of field in maser bulb. (Transition frequency (1.4 ± 0.2) kHz.)

7.0 Measurements of Relative Frequency

At this point the masers are operating at their nominal condition of pressure and field. Measurements of relative frequency can be made prior to starting the tuning procedure.

7.1 Measure frequency between masers.

7.2 Select, on basis of best performance, maser for controlling clock system and command this maser to be in control.

7.3 Turn on autotuner system timer and time code generator.

7.4 Check autotuner timer and time code generator signals.

7.5 Turn on Doppler cancelling receiver system.

7.6 Monitor voltages and currents in Doppler system.

7.7 Check performance of Doppler system.

7.8 Turn on Doppler system recording apparatus.

7.9 Compare ground based red shift output frequency from Doppler Cancelling System with output from satellite system. These should be equal except for a small phase lag due to radial acceleration of the satellite. The signals will contain a systematic frequency shift due to the as yet untuned condition of the satellite masers.

7.10 This data should be monitored for one more orbit to check the Doppler system and to get a first cursory look at the red shift between apogee and perigee. The magnetic field of the non-controlling masers and the beat frequency between all masers should be checked for 24-hour variations

8.0 Autotuning

The autotuning is now begun using the best operating maser, now in control of the system, as a reference oscillator.

8.1 Select maser to be tuned (if three masers are aboard).

8.2 Check beat between the two masers.

8.3 Raise source pressure on maser to be tuned.

8.4 Test and reset, if necessary, the high and low levels of r.f. excitation.

8.5 Check discharge intensity and color.

8.6 Check second I. F. output.

8.7 Check for gross offset in frequency between masers at high and low excitation.

8.8 Command reset reversible counter.

8.9 Command start of autotuner.

8.10 Check reversible counter operation.

8.11 Check status of 12-bit D. A. during one or more orbits--look for systematic 24-hour variations.

8.12 Repeat 8.1 to 8.11 for other maser.

8.13 Check beat between the two tuned masers and between these and the control maser for one or more orbits. Check stability and select most stable maser for control.

8.14 Switch control to this maser.

8.15 Repeat 8.1 to 8.11 for this maser.

8.16 Compare all relative maser frequencies in satellite.

8.17 Recheck magnetic fields of masers not in control.

8.18 Check all maser bulb temperatures.

8.19 If any maser seems out of tune, repeat autotuning procedure as in Section 8 above.

9.0 Preliminary Red Shift Comparisons

At this point the most accurate data taking phase of the experiment begins and comparisons of red shift modulation due to the eccentricity of the orbit with the average time red shift over the orbit can be begun. Data has been accumulated since phase 7.9 of the plan. The sequence of tuning is such as to retain as much as possible of the red shift information, upgrading the stability and precision of the clock output in such a way as to minimize the danger of losing the status quo at any given phase.

9.1 Observe data with autotuner operating on a maser that is not in control of the system. This should be done for several orbits.

9.2 Compare this data with data of masers that are not under autotune.

9.3 Decide whether autotuner should be used continuously and on which masers it should be used. Estimate the systematic 24-hour periodic effects (if any are observable) from the behavior of the autotuner D.A. output.

9.4 Repeat 8.1, 8.2 and 8.3 to get latest data on ground maser performance.

9.5 Test the magnetic field behavior with time of the two satellite masers not in control of the system. Compare these data with data obtained previously (see 6.24 and 7.10).

9.6 Select best maser on overall performance basis for control and switch over to this maser, if necessary.

9.7 Test state of tuning of masers not in control of system in both satellite and ground systems if the autotuner is not in continuous operation.